CENTRO DE INVESTIGACIÓN Y DESARROLLO
TECNOLÓGICO EN ELECTROQUÍMICA

Estudio de la reacción de evolución de hidrógeno, la reacción de oxidación de hidrógeno y la electrooxidación de metanol sobre Renio metálico
(Study of hydrogen evolution reaction, Hydrogen oxidation reaction and methanol electrooxidation on metallic Rhenium)

TESIS PRESENTADA POR:

I.Q. JOSE GUADALUPE RIVERA MORALES

PARA OBTENER EL GRADO DE:

MAESTRÍA EN ELECTROQUÍMICA

Noviembre, 2017

Centro de Investigación y Desarrollo Tecnológico en Electroquímica

REALIZADO POR:

I.Q. JOSE GUADALUPE RIVERA MORALES

DIRIGIDA POR

Dr. GERMÁN OROZCO GAMBOA

SINODALES

Dr. Fabricio Espejel Ayala _____
Presidente **Firma**

Dr. José Luis Jurado Baízaval _____
Secretario **Firma**

Dr. Raúl García García _____
Vocal **Firma**

Dr. Juan Manríquez Rocha _____
Suplente **Firma**

Resumen

El presente trabajo de tesis de Maestría en electroquímica pretende contribuir con conocimientos en el área de la electrocatálisis. Se estudió la reacción de evolución de hidrógeno (HER), la reacción de oxidación de hidrógeno (HOR) y la reacción de electrooxidación de metanol (MOR) sobre renio metálico. Estas reacciones han sido ampliamente estudiadas en cientos de materiales; sin embargo, existe muy poca información del desempeño de metal renio, lo que motivo el estudio. La literatura sobre el tema permite suponer que el renio tiene un buen desempeño para realizar ese conjunto de reacciones, aunque existe ambigüedad sobre si la reacción de evolución hidrógeno sobre el renio sigue o no el principio de Sabatier. Por otra parte, la literatura sobre estudios teóricos de reacciones de metanol propone que el renio participa como donador de oxígenos en el mecanismo para la electrooxidación de metanol; sin embargo no hay una contraparte experimental para verificar este postulado. Se ha realizado un estudio experimental electroquímico para determinar las corrientes de intercambio de las mencionadas reacciones sobre renio metálico. Se concluye que el renio sigue el principio de Sabatier respecto a la reacción de evolución de hidrógeno y que no tiene electroactividad para la electrooxidación de metanol como lo sugiere la literatura.

Abstract

The present master thesis project pretends to contribute with knowledge that helps to understand the three main reactions within the area of electrocatalysis. The hydrogen evolution reaction (HER), hydrogen oxidation reaction (HOR) and methanol electrooxidation reaction (MOR) were studied on metallic. This reactions has been widely studied on several materials. On the literature do not exist a lot information about the rhenium performance, this was the principal motivation for this study. The few studies predict a good performance of rhenium to perform this reactions, although there is ambiguity, if the hydrogen evolution reaction on rhenium follows or not the Sabatier principle. A theoretical study proposes that rhenium participate on the mechanism for the electrooxidation of methanol as oxygen donor, however there is no experimental evidence to verify this. Therefore an experimental study has been carried out to determine exchange currents for the HER on metallic rhenium. According with the experimental data obtained it is postulated that rhenium follows the Sabatier principle and dos not participate in the methanol electrooxidation.

Este trabajo fue realizado en el Centro de Investigación y Desarrollo Tecnológico en Electroquímica (CIDETEQ), bajo la dirección del Dr. Germán Orozco Gamboa

AGRADECIMIENTOS

Al Dr. Germán por su apoyo, dedicación, su conocimiento, su confianza depositada en mí y por darme la oportunidad de realizar la presente tesis de maestría.

A los sinodales por sus aportaciones, comentarios que han contribuido para el desarrollo de tesis de maestría.

Al CIDETEQ por brindarme la oportunidad de cursar un posgrado.

Al CONACYT a través del programa de becas nacionales por el apoyo económico otorgado durante estos dos años.

A Raúl, Mateo y a Jesús Alberto por ser mis compañeros dentro del grupo de investigación, su apoyo y sobre todo su amistad y confianza.

A todos los amigos, maestros y compañeros de laboratorio.

A mi familia por su comprensión y apoyo durante este tiempo.

A Dios, por estar junto a mí en cada proyecto, fortalecer mi confianza para poder terminar esta etapa de la vida.

Index

Index of figures

Index of Tables

About the project

Overview.

The central point in electrocatalysts is to develop high active, selective and stable materials. In order to produce this electrocatalyst is required enough knowledge of how an electrocatalyst functions, such as the reaction mechanism and active sites. Consequently, the goal is to provide experimental data about electrocatalytic materials and the analysis of these data contribute to the understanding the electrocatalyst activity.

In electrocatalysts is necessary to take account two principal reactions: 1) hydrogen evolution reaction (HER), 2) hydrogen oxidation reaction before study a new material for a determinate reaction in aqueous media. In this study a third reaction is added due the relevance for the main objective 3) methanol electrooxidation reaction (MOR). For metallic rhenium there are very few scientific articles about the HER, HOR and MOR; the few information about it shows contradictions about electroactivity of rhenium and this will be presented in the chapter I. From the literature it was identified several points that did not addressed completely or the information are unclear. In Chapter II Pourbaix and speciation diagrams were constructed using data selected from the literature. However, the Pourbaix and speciation diagrams for rhenium compounds and methanol species have not been reported before in literature and their interpretation provides information where several oxides on the surface could react with methanol and their products. It was calculate the exchange current of HER for the sixth period elements of the periodic table with basis in the work function and equation reported in literature to compare this calculated exchange current with the experimental data obtained in this work and in the literature. In addition, a theoretical pathway of the MOR was suggested with basis in free energy reported in literature. Consequently, a specific mechanism reaction of electrooxidation of methanol on rhenium can be suggested. Tables and figures, in chapter II, are not reported before in literature to study the system of Re as electrocatalyst for HER in acidic media or interpret the discrepancy for the exchange current value. The chapter III is divided in two parts: the first one, focused in the experimental determination of HER and HOR on metallic rhenium, meanwhile the second part, to quantified the influence of methanol on the HER and to study the electrooxidation of methanol on rhenium. Chapter IV enlisted twelve conclusions obtained in this work and suggestions for future directions.

Objectives.

General Objective.

The main objectives of the present thesis were: (1) the electrochemical study of metallic rhenium as electrocatalyst for hydrogen evolution reaction (HER) and hydrogen oxidation reaction (HOR) by the determinations of exchange current and (2) the methanol electrooxidation reaction (MOR) on metallic to determinate the rhenium activity for methanol.

Specific Objectives.

1. To determine the exchange current density of hydrogen evolution reaction on rhenium in acidic media and gas (N_2 and H_2).
2. To determine the influence of methanol on the hydrogen evolution reaction.
3. To determine the potentials and currents of the electrooxidation of methanol peak above on rhenium.
4. Perform an impedance study in potentials, where the hydrogen evolution reaction on rhenium occurs.

Hypothesis.

According with the literature it can be stablished three questions about the for rhenium for HER, HOR and MOR:

- ¿Metallic rhenium follows the Sabatier principle for HER?.
- ¿The exchange current density of HOR is equal to exchange current density of HER because these reactions are reversible?.
- ¿Metallic rhenium participate in the bi-functional mechanics in the MOR?.

List of Publications and contributions.

Electrooxidation of Methanol by Metallic Rhenium.

RIVERA, José, GARCÍA, Raúl and OROZCO, Germán. Electrooxidation of Methanol by Metallic Rhenium. ITP Journal 2015, 1-1: 73-77.

Abstract

There is only a theoretical study of the methanol electrooxidation on metallic rhenium; this motivates the experimental determination of electrochemical oxidation of this substance. The voltammograms at potentials between -0.20 V to 0.80 V vs RHE are similar in presence of methanol that the voltammograms in solutions without this alcohol. At these potentials was observed a formation of thin layer of superficial oxides. The formation of soluble ReO_4, occurs at potentials around 0.88 V vs RHE in presence or absent of methanol. These results were observed at different temperatures and scan rates. Then, the effects of methanol are insignificant and consequently the metallic Rhenium does not have activity for the methanol electrooxidation as theoretically was predicted. On the other hand, the current density of hydrogen formation faithfully follows the Sabatier principle. To be precise the density current is in the magnitude order of 10^{-7} Acm^{-2}, which is three orders of magnitude inferior that the data reported in several textbooks.

Contribution

The original idea came from my supervisor to study the methanol electrooxidation on rhenium electrode in acidic media, to determinate the electrocatalytic activity of rhenium for the methanol electrooxidation.

My responsibility was designed an experimental protocol and collected the experimental data. My supervisor provided direction, guidance about the results, help to write and edit the manuscript

Impedance spectra of the cathodic hydrogen evolution reaction on polycrystalline rhenium.

Garcia-Garcia, R., Rivera, J. G., Antaño -Lopez, R., Castañeda-Olivares, F., & Orozco, G. Impedance spectra of the cathodic hydrogen evolution reaction on polycrystalline rhenium. International Journal of Hydrogen Energy, 41(8) (2016) 4660-4669

Abstract

The cathodic behavior of metallic rhenium was studied potentiodynamically in acid media. The impedance spectra were analyzed to determine the behavior of the hydrogen evolution reaction (HER) on polycrystalline rhenium. Our results show that the electrocatalytic behavior of the metallic rhenium towards the HER follows the principle of Sabatier. However, during the last years, volcano plots in textbooks show that platinum and rhenium have the same performance for the HER. The literature on HERs does not consider the formation of the rhenide anion, though polarographic studies have proposed the formation of the rhenide anion. However, the impedance spectra do not support the formation of this rhenide anion. Specifically, only one single charge transfer resistance was detected in the spectra, and consequently, the HER is the unique process in this range of potentials. The features of the impedance spectra were related to the changes of the resistance of the charge transfer, which corresponds to the HER on metallic rhenium. The parameters of the Randles equivalent circuit fulfill the impedance characteristics of the HER on this metal.

Contribution

I prepared the experimental setup, carried the electrochemical impedance measurements, collected analyzed the data. My supervisor wrote the manuscript provided direction throughout the research work and review of the manuscript with the others authors.

¿Es el Renio tan buen electrocatalizador como el platino para las reacciones de hidrógeno?

R. García-García, J. G. Rivera, G. Ortega-Zarzosa, G. Orozco, ¿Es el Renio tan buen electrocatalizador como el platino para las reacciones de hidrógeno? 8th Meeting of The Mexican Section of the Electrochemical Society, Mexico (2015) CAE-06.

Resumen (Abstract).

La electrocatálisis se explica con base en las curvas de volcán. Estos gráficos establecen la relación entre la densidad de corriente de intercambio (j_0) y la energía libre de adsorción de hidrógeno sobre la superficie del electrodo (ΔG). Este gráfico para la reacción de formación de hidrógeno gaseoso (Hydrogen Evolution Reaction) es mostrado ampliamente en la literatura, pero sobre todo en libros de texto. Cualquier nuevo estudiante del área de electrocatálisis observa que la mayoría de los metales siguen muy bien la tendencia marcada por los ramales de ascenso y descenso, es decir, existe poca dispersión de los datos. Sin embargo, es muy notorio que el Renio no sigue rigurosamente el principio de Sabatier. Por lo tanto, la actividad electrocatalítica del Renio ha sido una excepción durante mucho tiempo. Nuestra investigación establece que los valores de la densidad de corriente de intercambio (j_0) usados en la literatura son incorrectos, por lo tanto la reacción de hidrógeno sobre Renio sigue el principio de Sabatier según los valores determinados en esta investigación.

Contribution

I had the responsibility to carry the polarizations curves and collected the experimental data. I write majority of the manuscript.

Chapter I

Introduction

1.1 Rhenium general chemistry.

Masataka claimed on 1908, that a new element called Nipponium had been isolated from element 43. However until 2004, it was revealed that he had isolated rhenium. This element was re-discovered by Walter Noddack, Ida Tacke and Otto Berg in 1925 and they named it rhenium after the river Rhine in Germany [1].

Sometimes in literature rhenium is classified as a refractory metal because, it does not fit in any other classification [2–5]. This metal is strong, ductile and possesses an hcp crystalline structure. It has a very high density (21.0 gcm^{-3}) and its melting point is at 3180 °C. Rhenium has the following electronic configuration [Xe]$4f^{14}5d^{5}6s^{2}$, it shows a large range of oxidation states (+7, 6+, 5+, 4+, 3+, +2, +1, 0 and –1) more than any other known element. Roughly 0.7−1.0 parts per billion of rhenium can be found on the earth's crust. In 2015 the rhenium world's production was about 46,000 Kg. and despite the shortage production its compounds have unique properties; rhenium diboride for instance, is one of the hardest of all known substances. Sims et. al. indicated that rhenium is a considerable metal of considerable interest, actually the main uses of rhenium are in superalloys, platinum-rhenium catalysts (to produce high-octane, lead-free gasoline), contact points, thermocouples, flashbulbs, electromagnets, heating elements, vacuum tubes [2–4,6], among others.

1.2 The state of the art in Hydrogen Evolution Reaction and Hydrogen Oxidation Reaction on Rhenium.

Due to its scarcity, few studies of rhenium in electrocatalysis are known and these studies indicated that Re has an activity similar that platinum in the Hydrogen Evolution Reaction (HER).

Studies of rhenium as electroctalyst exist in literature [7,8], however, there is a huge discrepancy between the data reported [7–11]. The key points under discussion for the electroactivity of Re in the HER are the following:

1. The volcano plot reported by Trasatti [9] used the standard exchange current density (j_0) reported by Pecherskaya [7] in acid media. On the other hand, the volcano plotted by Appleby [11] used the data from Joncich [8], who studied the HER in hydrochloric acid. The kinetic parameters values indicated by Pecherskaya [7] and Joncich [8] for rhenium towards the HER display a difference of the three orders of magnitude. Then, some data of the j_0 implies that rhenium does not rigorously follow the Sabatier principle.

García [12] suggested that the metallic Re follows the Sabatier principle, but new data are necessary to support this claim.

2. It has proposed that two types of hydrogen adsorption process occur on the metal surface, firstly one with high adsorption energy which follows the Sabatier principle and therefore is kinetically slow and the second one corresponds to the adsorption of protons close to zero energy, which is kinetically faster than the first one[13]. Furthermore, the binding energies of atomic hydrogen to surface and subsurface on several metals were calculated by Greeley [14]. Additionally, Krasikov [15] explains the behavior of polarization curves at very high cathodic polarization potentials with basis the formation of atomic hydrogen on the metal surface and subsurface. However, it is not clear yet if the formation of atomic Hydrogen on the rhenium subsurface is a feasible process, Greeley [14] did not report data related to the binding energies. García [12], mentioned that is it difficult to sustain the two different adsorption energies for hydrogen on metallic rhenium using potential–log current plots. This issue will be revised in this study by means of Electrochemical Impedance Spectroscopy (EIS) because this technique allows to separate the contributions of each process.
3. Joncich [8] reported that the mean activation enthalpy at the equilibrium potential was related to Tafel reaction forward and backward steps.
4. In 1992, Trassati [16] reported a value of 30 mVdecade^{-1} for the Tafel slope of Re in acid media, this value was also obtained by Krasikov [10], in 1981. The value shows a notable exception, because 30 mVdecade^{-1} is observed only for platinum at low polarization [16]. A few years after, in 1998, Szabó [17] obtained also the same value (31 mVdecade^{-1}), but in this case for rhenium electrodeposited on platinum. Szabó [17] concluded that Hydrogen overvoltage is not greatly related to electrodeposited rhenium, in fact, the Tafel slope for HER on platinum covered with rhenium-oxide is the same than that of bare platinum. García [12] presented in his study that at low polarization the Tafel slope value was set around 60 mVdecade^{-1}. This is consistent with the data reported by Krasikov [10] on electrodeposited rhenium. The surfaces obtained by electrodeposition of soluble oxides are a mixture of oxides and metallic Re [17–19]. Krasikov [15] claimed that in small amounts of rhenium oxides, the HER the reactions can be as follows:

$$ReO_x + e^- \rightarrow ReO_x^- \qquad \text{Eq. 1.1}$$

$$2ReO_x^- + 2H_3O^+ \rightarrow 2ReO_x + H_2 + 2H_2O \quad \text{Eq. 1.2}$$

In this regard, Vargas-Uscategui [19] commented that a greater concentration of Re (VII) oxide compare to the concentration of Re (IV) oxide, would cause an increment in the HER rate. According whit Krasikov [10,15] and Szabó [17] observations, it can be inferred that the different rhenium oxides generate a dissimilar influence over the Tafel slopes. On the other hand, metallic rhenium possesses a Tafel slope of 60 mVdecade^{-1} [12,20].

5. Pourbaix diagram show that the formation of rhenide anion (Re^-) take place at the same potential as the HER [21]. Subsequently, the metal dissolution current could be related by the apparent formation of Re^- and as consequence produces an overestimation of the j_0 value. Nowadays, this anion still appears in the potential-pH diagrams of rhenium [22]. In 1999, Kohlíčková [23] determined the concentration of Re species in solution using polarography as analytical technique and the Re^- and was considered among the Re species analyzed. García [12], Li [24] and Ellis [25] do not particularity support the existence of this anion in their experimental conditions, while Krasikov [15] postulated the possibility of rhenide and rhenium hydride formation. It is important to mention that Re^- only appears at very high cathodic potentials and in the presence of amalgams. Nevertheless, the standard potential of the formation reaction of this anion will be mentioned bellow [26], considering that it is important to clarify the area on the Pourbaix diagram.
6. Chun et. al. [20] assigned a pair of peaks observed at 0.21 V to the under-potentially deposited hydrogen (UPD-H) process. Conversely, Gómez et al. [27] assign this peaks to the Eq. 1.3 reaction, whose equilibrium potential is 0.258 V at pH 0.3 according to equation Eq. 1.4.

$$ReO_4^- + 4H_2O + 8e^- \rightarrow Re^- + 8OH^- \quad \text{Eq. 1.3}$$

$$E = -0.1 - 0.0591 \log a_{Re^-} \quad \text{Eq. 1.4}$$

7. Chun et al. [20] calculated the Langmuir adsorption isotherms of hydrogen on rhenium using the patterns of the phase-shift versus the potentials at optimum intermediate

frequency (phase-shift method). This approach was refuted by Lasia [28], which along with Chun [20], based their discussion on the premise that platinum and rhenium have identical electroactivity towards the HER. The phase shift method requires a proper discussion using reliable kinetic parameters, as a result, this motivated to present a study included in this work (chapter III). It was observed that the results found are in agreement with Randles as an equivalent circuit [29].

8. In 2016, Krasikov [15] reviewed Russian literature available for HER on Re surfaces, these surfaces were obtained by electrodeposition or vapor deposition. In the 1980's a noteworthy effort to determinate the mechanism for HER on these rhenium surfaces was made, data that unfortunately was not reported in literature in English [17,19]. The mechanics include, the stage of protons discharge followed by the absorption into a subsurface site and diffusing through the metal subsurface layer, a further transfer from the subsurface state to the adsorbed state and finally a recombination of hydrogen atoms to form molecular hydrogen, this support the commented by Szabó [17] in 1998, who postulated that the absorption of hydrogen atoms by rhenium oxides deposited on platinum surface is suitable.
9. The experimental exchange current densities compiled by Trasatti [9] and Parsons [30] were used to plot the volcano curves commonly included in introductory courses textbooks, for example [31], with the suggestion that metallic rhenium does not follow the Sabatier principle. Nevertheless, several kinetic modeling for HER on polycrystalline or single crystal based on the assumption that rhenium and platinum have the same performance towards the HER [32–38]. This scenario also motivated this study, since a suitable discussion needs the most reliable kinetic parameters.

1.3 The exchange current densities of HER and work functions of metals.

Since 1930, the area of electrocatalysis was focused on the study of the Hydrogen Evolution Reaction and Hydrogen Oxidation Reaction (HOR). Both reactions are extensively studied in literature [9–16,30–34,36–43]. In this regard, the Sabatier principle postulated for heterogeneous catalysis was introduced by Trasatti [9] in relation to the HER in electrocatalysis. This idea postulated the following; if the Metal-Hydrogen (M-H) bond energy is too weak, there will be no adsorption, therefore any electrocatalytic effect is expected. Another possible case is that if this M-H energy is strong, the surface will be

totally covered and blocked, subsequently, the metal can no longer act as an electrocatalyst. The optimum electrocatalyst is found, in an intermediate level; there is a consensus that the maximum electrocatalytic activity correspond to zero M-H energy [30]. Furthermore, in 1982 Appleby and Kita [11] performed an effort to enlist the exchange current densities for the HER of as many metals as possible. These authors established a periodicity behavior of j_0, which is the strongest feature in the Periodic Table: all properties of elements change periodically, including the exchange current density for the HER. In recent times, the volcano curve has been rediscovered because new data of the adsorption energy of hydrogen on several metals have been calculated using for example, the density functional theory [34], therefore there is a discussion about the trustworthiness of the calculated Gibbs free energies of adsorption (ΔG) for the HER on the new volcano plots [35].

In 1957, Bockris and Conway [42] established a linear behavior between log j_0 and the metal work function (Φ), after that, in 2002, Harinipriya and Sangaranarayanan [43] calculated the j_0 for HER on several metals from Φ values, including rhenium. The j_0 experimental value for HER on rhenium determinated by Pecherskaya [7] and Joncich [8] display a difference of three orders of magnitude and therefore evidently there is an inconsistency between the experimental exchange current density of polycrystalline rhenium and the exchange current calculated by Harinipriya and Sangaranarayanan [43], leaving unfinished experiments that will encounter a possible solution once new and reliable kinetic parameter are found.

1.4 Methanol activity on metallic Rhenium and their alloys.

It has been observed that j_0 for HER and HOR on several metals may vary slightly due to the medium. In this regard, the aqueous methanol has an influence on the HER. Different adsorbed species have been suggested based on infrared spectroscopy data [44–46]. It is well-know that the inhibition of HER in presence of methanol is due to the adsorbed species, for example, the hydrogen electrooxidation on several metals is suppressed by the methanol poisoning intermediates. In 1967, Cathro [47] studied the electrooxidation of methanol and found a low performance of rhenium towards the electrooxidation of methanol. The rhenium electrodes and the influence of methanol in the HER have not been reported widely in the literature. It could be a competition for adsorption sites between the proton and methanol in several metals and rhenium is included. Some works

reported the influence of methanol in the HER. This study was cited by [48–50], but the low performance of rhenium had not been confirmed. On the other hand, Ferrin [51] performed a Functional Density Theory (DFT) study for methanol electrooxidation on 12 transition metals, including rhenium. In this regard, the Cathro [47] and Ferrin [51] results can be compared to determine the real behavior of rhenium for the electrooxidation of methanol, as previously mentioned, new and experimental results are needed to sustain the electrocatalytic activity for methanol electrooxidation.

Shropshire [52] commented that methanol electrooxidation on platinum can be promoted by soluble rhenium compounds. Besides, the electrocatalytic activities of rhenium oxides and rhenium alloys towards the methanol are very diverse. A synergistic effect was detected in PtReSn [53–55], PtRuRe [56] and PtRe [47,56,57] alloys. However, other studies have suggested that the electrooxidation of methanol on PtRe alloys was lower than PtRu alloys [58–61], for example Grgur, has made speculations about rhenium, specifically that sites are poorly for hydrogen electrooxidation, to explain the observed polarization curves of PtRe alloy, which follows the Pt comportment, more than the rhenium one, that is, there is not a rhenium influence apparently . In 2010, Narayanan [62] suggests that ternary rhenium alloys can perform the methanol electrooxidation, however, no experimental result was provided to support this assessment.

The performance of Pt-based bimetallic electrocatalysts has been extensively revised [63–65]. Two mechanisms have been proposed for the enhanced electrocatalytic activity associated with these binary and ternary electrocatalysts. One was the “bifunctional mechanism” and the other one is the “electronic effect”, where foreign atoms modify the electronic structure of nearby Pt atoms and then they weaken the adsorption of monoxide carbon on the surface therefore facilitating the removal of monoxide carbon. The bifunctional effect is believed to occur when the foreign atom provides $-OH_{(ads)}$ to Pt for the complete oxidation of CO to CO_2. This effect was proposed in heterogeneous catalysis in steam environment for PtRe alloys [66–70].

Based on the references quoted above [47,52–57,61], it was possible to establish the hypothesis that the electrooxidation of methanol on rhenium was similar than the mechanism observed in platinum metals group. The electrodeposition of rhenium in hydrochloric acid media with methanol was studied by Szabó and Bakos [70,71]. This study postulates that the H_{ads}, formed by dehydrogenation steps of CH_3OH on platinum surface, can react with ReO^{4-} , increasing the quantity of rhenium electrodeposited onto

platinum surface. Szabó and Bakos [70] commented that the mechanism for the electrooxidation of methanol in rhenium deposited on platinum surface was different from the mechanism of oxidation on rhenium-free platinum surface, the peak of electrooxidation of CO_{ads} was smaller on rhenium-covered surface, which was caused by the reduction of the platinum surface area, because of the presence of the electrochemical inactive rhenium-covered surface Hence, the aim of this study is to determinate the possible peak potentials and currents for the methanol electrooxidation.

1.5 References.

[1] Scerri E. Recognizing rhenium. Nat Chem 2010;2:598.

[2] Désirée E. Polyak. Rhenium. Miner. Commod. Summ., 2016, 136–7.

[3] Désirée E. Polyak. Rhenium [Advance Release]. U.S. Geol. Surv. MINE RALS Yearb., U.S. Geological Survey; 2014, 62.1-62.6.

[4] Jhon D. Rhenium: A rare metal critical to modern transportation, No. 2014-3101. US Geological Survey, 2015.

[5] Naor A, Eliaz N, Gileadi E, Taylor S. Properties and applications of rhenium and its alloys. AMMTIAC Q 2010;5:11–5.

[6] Sims CT, Craighead CM, Jaffee RI, N. GD, Kleinschidt WW, Nexsen WE, et al. Investigations of Rhenium, WADC Technical report 54-371, Battelle Memorial Inst, Columbus OH, 1956.

[7] Pecherskaya AG, Stender V V. Potentials of the evolution of hydrogen in acid solutions. Zhurnal Fiz Khimii 1950;24:856–9.

[8] Joncich MJ, Stewart LS, Posey FA. Hydrogen Overvoltage on Rhenium and Niobium Electrodes. J Electrochem Soc 1965;112:717.

[9] Trasatti S. Work function, electronegativity, and electrochemical behaviour of metals. III. Electrolytic hydrogen evolution in acid solutions. J Electroanal Chem 1972;39:163–84.

[10] Krasikov VL, Varypaev VN. Electrochemical behaviour of rhenium-graphite electrode. Zhurnal Prikl Khimii 1980;53:1061–4.

[11] Appleby AJ, Chemla M, Kita H, Bronoel G, Bard A. Encyclopedia of Electrochemistry of the Elements Volume. New York, NY: M. Dekker New York; 1982.

[12] Garcia-Garcia R, Ortega-Zarzosa G, Rincón ME, Orozco G. The Hydrogen Evolution Reaction on Rhenium Metallic Electrodes: A Selected Review and New Experimental Evidence. Electrocatalysis 2015;6:263–73.

[13] Schmickler W, Santos E. Hydrogen reaction and electrocatalysis. Interfacial Electrochem. 2nd ed., Berlin, Heidelberg: Springer Berlin Heidelberg; 2010, p. 166–7.

[14] Greeley J, Mavrikakis M. Surface and Subsurface Hydrogen: Adsorption Properties on Transition Metals and Near-Surface Alloys. J Phys Chem B 2005; 109:3460–71.

[15] Vladimir L. Krasikov. A new Approach to Mechanics of Hydrogen Evolution Reaction on Rhenium: 3D-Recombination,. Bull Saint Petersbg State Inst Technol (Technical Univ 2016;60:24–32.

[16] Trasatti S. Electrocatalysis of hydrogen evolution: progress in cathode activation. In: Gerischer H, W. Tobias C, editors. Adv. Electrochem. Sci. Eng., vol. 2, New York: VCH Verlagsgesellschaft mbH Weinheim; 1992, 6,10,20.

[17] Szabó S, Bakos I. Study of rhenium deposition onto Pt surface with electrochemical methods. Prep Catal VII, Proc 7th Int Symp Sci Bases Prep Heterog Catal 1998;118:269–76.

[18] Eliaz N, Gileadi E. Induced Codeposition of Alloys of Tungsten, Molybdenum and Rhenium with Transition Metals. In: Vayenas CG, White RE, Gamboa-Aldeco ME, editors. Mod. Asp. Electrochem., New York, NY: Springer New York; 2008, 191–301.

[19] Vargas-Uscategui A, Mosquera E, Chornik B, Cifuentes L. Electrocatalysis of the hydrogen evolution reaction by rhenium oxides electrodeposited by pulsed-current. Electrochim Acta 2015;178:739–47.

[20] Chun J, Jeon S, Kim N, Chun J. The phase-shift method for determining Langmuir and Temkin adsorption isotherms of over-potentially deposited hydrogen for the cathodic evolution reaction at the poly- aqueous electrolyte interface. Int J Hydrogen Energy 2005;30:485–99.

[21] De Zoubov N, Pourbaix M, Pourbaix M. Rhenium. Atlas Electrochem. Equilibria Aqueous Solut., NACE: Houston, TX; 1974, 300–6.

[22] Srivastava RR, Lee J chun, Kim M seuk. Complexation chemistry in liquid-liquid extraction of rhenium. J Chem Technol Biotechnol 2015;90:1752–64.

[23] Kohlíčková M, Jedináková-Křížová V, Horejš M. Influence of technetium and rhenium speciation on their sorption on natural sorbents. Czechoslov J Phys 1999;49:695–700.

[24] Li C, Agarwal J, Schaefer HF. The remarkable $[ReH_9]^{2-}$ dianion: Molecular structure and vibrational frequencies. J Phys Chem B 2014;118:6482–90.

[25] Ellis JE. Adventures with substances containing metals in negative oxidation states. Inorg Chem 2006;45:3167–86.

[26] Bard AJ, Parsons R, Jordan J. Standard potentials in aqueous solution. Marcel Derkker; 1985.

[27] Gómez J, Gardiazábal JI, Schrebler R, Gómez H, Córdova R. Electrochemical behaviour of rhenium in aqueous solution. J Electroanal Chem 1989;260:113–26.

[28] Lasia A. Comments on “the phase-shift method for determining Langmuir adsorption isotherms of over-potentially deposited hydrogen for the cathodic H_2 evolution reaction at poly-Re/aqueous electrolyte interfaces” [Hydrogen Energy 30 (2005) 485-499]. Int J Hydrogen Energy 2005;30:913–7.

[29] Garcia-Garcia R, Rivera JG, Antaño-Lopez R, Castañeda-Olivares F, Orozco G. Impedance spectra of the cathodic hydrogen evolution reaction on polycrystalline rhenium. Int J Hydrogen Energy 2016;41:4660–9.

[30] Parsons R. Volcano Curves in Electrochemistry. In: Santos E, Schmickler W, editors. Catal. Electrochem. From Fundam. to Strateg. Fuel Cell Dev., Hoboken, New Jersey: John Wiley & Sons, Inc.; 2011, 1–15.

[31] Krstajic N. Hydrogen Evolution Reaction. In: Kreysa G, Ken-ichiro O, Savinell RF, editors. Encycl. Appl. Electrochem., New York, NY: Springer New York; 2014, 1039–44.

[32] Santos E, Quaino P, Schmickler W. Theory of electrocatalysis: hydrogen evolution and more. Phys Chem Chem Phys 2012;14:11224. doi:10.1039/c2cp40717e.

[33] Jaksic MM. Volcano plots along the periodic table, their causes and consequences on electrocatalysis for hydrogen electrode reactions. J New Mater Electrochem Syst 2000;3:153–68.

[34] Quaino P, Juarez F, Santos E, Schmickler W. Volcano plots in hydrogen electrocatalysis – uses and abuses. Beilstein J Nanotechnol 2014;5:846–54.

[35] Conway BE, Jerkiewicz G. Relation of energies and coverages of underpotential and overpotential deposited H at Pt and other metals to the `volcano curve' for cathodic H_2 evolution kinetics. Electrochim Acta 2000;45:4075–83.

[36] Nørskov JK, Bligaard T, Logadottir A, Kitchin JR, Chen JG, Pandelov S, et al. Trends in the Exchange Current for Hydrogen Evolution. J Electrochem Soc 2005;152:J23.

[37] Schmickler W, Trasatti S. Comment on "Trends in the Exchange Current for Hydrogen Evolution" [J. Electrochem. Soc., 152, J23 (2005)]. J Electrochem Soc 2006;153:L31–2.

[38] Nørskov JK, Bligaard T, Logadottir A, Kitchin JR, Chen JG, Pandelov S, et al. Response to "Comment on 'Trends in the Exchange Current for Hydrogen Evolution' [J. Electrochem. Soc., 152, J23 (2005)]." J Electrochem Soc 2006;153:L33.

[39] Skúlason E, Tripkovic V, Björketun ME, Gudmundsdóttir S, Karlberg G, Rossmeisl J, et al. Modeling the Electrochemical Hydrogen Oxidation and Evolution Reactions on the Basis of Density Functional Theory Calculations. J Phys Chem C 2010;114:18182–97.

[40] Li H, Lee K, Zhang J. Electrocatalytic H_2 Oxidation Reaction. PEM Fuel Cell Electrocatal. Catal. Layers, London: Springer London; 2008, 135–64.

[41] Santos E, Schmickler W. Electronic interactions decreasing the activation barrier for the hydrogen electro-oxidation reaction. Electrochim Acta 2008;53:6149–56.

[42] Conway BE, Bockris JO. Electrolytic Hydrogen Evolution Kinetics and Its Relation to the Electronic and Adsorptive Properties of the Metal. J Chem Phys 1957;26:532.

[43] Harinipriya S, Sangaranarayanan M V. Influence of the Work Function on Electron Transfer Processes at Metals: Application to the Hydrogen Evolution Reaction. Langmuir 2002;18:5572–8.

[44] Iwasita T, F.C. N. In-Situ Infrared Fourier Transform Spectroscopy: A Toll to Caracterize the Metal-Electrolyte Interface at a Molecular Level, Volume 4. In: Gerischer H, W. Tobias C, editors. Adv. Electrochem. Sci. Eng., New York: VCH Publishers, Inc. (New York) & VCH Verlagsgesellschaft mbH, Weinheim (Germany); 1995.

[45] Iwasita T, Iwasita, T. Methanol and CO electrooxidation. Handb. Fuel Cells, Chichester, UK: John Wiley & Sons, Ltd; 2010.

[46] Osawa M. Chapter 7 – Electrocatalytic Reactions on Platinum Electrodes Studied by Dynamic Surface-Enhanced Infrared Absorption Spectroscopy (SEIRAS). In-situ Spectrosc. Stud. Adsorpt. Electrode Electrocatal., 2007, 209–46.

[47] Cathro KJ. Use of platinum-rhenium catalysts for the oxidation of aqueous methanol Low-temperature fuel cell operating on water- soluble organic fuels X-ray diffraction and electron microscope studies of narcissus mosaic virus , and comparison with potato virus X. Electrochem Technol 1967;5:441–5.

[48] Cathro KJ. The Oxidation of Water-Soluble Organic Fuels Using Platinum-Tin Catalysts. J Electrochem Soc 1969;116:1608.

[49] Cathro KJ. Fuel Control in Methanol-Air and Formaldehyde-Air Fuel Cell Systems. J Electrochem Soc 1971;118:1523.

[50] Attwood PA, McNicol BD, Short RT. The electrocatalytic oxidation of methanol in acid electrolyte: preparation and characterization of noble metal electrocatalysts supported on pre-treated carbon-fibre papers. J Appl Electrochem 1980;10:213–22.

[51] Ferrin P, Nilekar AU, Greeley J, Mavrikakis M, Rossmeisl J. Reactivity descriptors for direct methanol fuel cell anode catalysts. Surf Sci 2008;602:3424–31.

[52] Shropshire JA. Catalysis of the Electrochemical Oxidation of Formaldehyde and Methanol by Perrhenate. J Electrochem Soc 1967;114:773.

[53] Weeks CH. Compatibility of Battery Materials with Fuel Cell Catalysts. J Electrochem Soc 1970;117:410.

[54] Goel J, Basu S. Pt-Re-Sn as metal catalysts for electro-oxidation of ethanol in direct ethanol fuel cell. Energy Procedia 2012;28:66–77.

[55] Tayal J, Rawat B, Basu S. Effect of addition of rhenium to Pt-based anode catalysts in electro-oxidation of ethanol in direct ethanol PEM fuel cell. Int J Hydrogen Energy 2012;37:4597–605.

[56] Liu F, Yan Q, Zhou WJ, Zhao XS, Lee JY. High regularity porous oxophilic metal films on Pt as model bifunctional catalysts for methanol oxidation. Chem Mater 2006;18:4328–35.

[57] Janssen MMP, Moolhuysen J. Binary systems of platinum and a second metal as oxidation catalysts for methanol fuel cells. Electrochim Acta 1976;21:869–78.

[58] Beden B, Kadirgan F, Lamy C, Leger JM. Electrocatalytic oxidation of methanol on platinum-based binary electrodes. J Electroanal Chem Interfacial Electrochem 1981;127:75–85.

[59] Grgur BN, Markovic NM, Ross PN. Electrooxidation of H_2, CO and H_2/CO mixtures on a well-characterized Pt-Re bulk alloy electrode and comparison with other Pt binary alloys. Electrochim Acta 1998;43:3631–5.

[60] Liu Z, Kang S, Shamsuzzoha M, Nikles DE. Synthesis and characterization of PtRe alloy nanoparticles as electrocatalysts for methanol oxidation. J Nanosci Nanotechnol 2010;10:4266–72.

[61] Anderson AD, Deluga GA, Moore JT, Vergne MJ, Hercules DM, Kenik EA, et al. Preparation of Pt-Re/Vulcan Carbon Nanocomposites Using a Single-Source Molecular Precursor and Relative Performance as a Direct Methanol Fuel Cell Electrooxidation Catalyst. J Nanosci Nanotechnol 2004;4:809–16.

[62] Narayanan SR, Whitacre JF. Low Pt content direct methanol fuel cell anode catalyst: nanophase PtRuNiZr 2010.

[63] Anderson AB, Grantscharova E, Seong S. Systematic Theoretical Study of Alloys of Platinum for Enhanced Methanol Fuel Cell Performance. J Electrochem Soc 1996;143:2075–82.

[64] Gyenge E. 04 - Electrocatalytic Oxidation of Methanol, Ethanol and Formic Acid. PEM Fuel Cell Electrocatal Catal Layers 2008:165–285.

[65] González ER, Ticianelli EA, Antolini E. Platinum-Based Supported Nanocatalysts for Oxidation of Methanol and Ethanol. Catal Electrochem From Fundam to Strateg Fuel Cell Dev 2011:453–85.

[66] King DL, Zhang L, Xia G, Karim AM, Heldebrant DJ, Wang X, et al. Aqueous phase reforming of glycerol for hydrogen production over Pt-Re supported on carbon. Appl Catal B Environ 2010;99:206–13.

[67] Zhang L, Karim AM, Engelhard MH, Wei Z, King DL, Wang Y. Correlation of Pt-Re surface properties with reaction pathways for the aqueous-phase reforming of glycerol. J Catal 2012;287:37–43.

[68] Azzam KG, Babich I V., Seshan K, Lefferts L. Role of Re in Pt-Re/TiO_2 catalyst for water gas shift reaction: A mechanistic and kinetic study. Appl Catal B Environ 2008;80:129–40.

[69] Ciftci A, Ligthart DAJM, Sen AO, Van Hoof AJF, Friedrich H, Hensen EJM. Pt-Re synergy in aqueous-phase reforming of glycerol and the water-gas shift reaction. J Catal 2014;311:88–101.

[70] Szabó S, Bakos I. Rhenium deposition onto platinum surface by reduction of perrhenic acid with methanol in hydrochloric acid media. React Kinet Catal Lett 1998;65:259–63.

[71] Szabó S, Bakos I. Rhenium deposition on platinum surface by reduction of perrhenic acid with methanol. React Kinet Catal Lett 1997;62:267–71.

Chapter II

Theory

2.1 Introduction.

The Chapter I discusses historical background studies of rhenium compounds towards the hydrogen evolution reaction. Additionally, the state of the art for the electrooxidation of methanol on rhenium surfaces was described. In this chapter, the Pourbaix and speciation diagrams for rhenium compounds and methanol species were built, based on the thermodynamics data to understand more exactly the system were Re is going to be analyzed for the HER. On the other hand, the theoretical studies used several assumptions for the development of the equations about metals electroactivity towards HER. In this chapter also a guide of the main equations of electroactivity will be presented. It was calculate the exchange current density considered with basis the Gibbs energy of activation for HER and work functions of metals to In this way, our study introduced concepts that help to understand the hydrogen reactivity. In addition, it is important to mention that some theoretical studies provide information which allows to separate the competing reaction pathways. Consequently, a specify mechanism reaction of electrooxidation of methanol on rhenium can be suggested.

2.2 The Rhenium predominance diagram in aqueous non-complexing environments.

Rhenium alloys are used to produce lead-free and high-octane gasoline, jet engine components, thermocouples, heating elements, temperature controls, vacuum tubes and Xray tubes, among others. Therefore, it is necessary to predict the chemical species which can be formed by the corrosion process in working conditions, it is also necessary to predict the nature of the rhenium electrode surface. Due to the latter, the predominance diagrams are constructed considering the thermodynamic stability of the metal compounds and species in aqueous solution. In the case of the rhenium-water system at 25 °C, from Pourbaix [1] were obtained the equations for a potential-pH diagram considering solid substances to Re, Re_2O_3, ReO_2, ReO_3 and Re_2O_7; Re^{3+}, ReO_4^- as aqueous solution. Similar diagrams have been constructed by Magge [2], Giraudeau [3], Darab [4], Takeno [5], García [6], Srivastava [7] and Zhulikov [8].

There are few studies focused on the corrosion and electrochemical behavior of metallic rhenium [3,9–11]. These works suggested that the total metal dissolution produces the perrhenate ion, this stage is proceeded by the formation of several intermediates compounds with various oxidation states including rhenide ion (Re^-). Magee [2] describes

the polarography studies of the perrhenate ion reduction made along three decades [12-27]. In 1999, Kohlíčková [29] assumed the formation of Re^- to describe the polarographic behavior of soluble rhenium. To support the formation of Re^-, Magee [2] also describes the formation of Re^- by the reduction of 8-electrons (Eq. 1.3).

The formation of rhenide ion potentials are included in the literature, for example [30-32], in 1989, Bratsch [33], commented that the standard potentials correspond to the unknown rhenium hydride rather than to the rhenide ion (Eq. 2.1). The Nernst equation (Eq. 1.4) predicted that the potential of the reaction is close to the thermodynamic potential of the Hydrogen evolution reaction (HER) in aqueous media.

$$Re + e^- \rightarrow Re^- \qquad \text{Eq. 2.1}$$

Krasikov [34] commented that the rhenide ion formation can be observed experimentally only at very high cathodic potentials, for example, while reducing perrhenates by zinc amalgam in acid media. However, no rhenide anion formation was observed in the electrodeposition of rhenium from acid perrhenates solutions. In 2014, Li [35] briefly describes the history of Re^-, which is confused with the soluble potassium rhenium hydride (ReH_9^{2-}). García et. al. [6] did not find experimental evidence of the presence of this anion. In this context, it can be mentioned as Ellis [36] did, that the formation of this anion was improbable in aqueous solutions. The confusion with the polarography studies arises from the disproportionate reactions of electrodeposited oxides. In fact, the electroreduction of ReO_4^- involves electrochemical and chemical steps [37-39]. The formation of rhenium bronze can be also postulated; however, it is not yet characterized. The reduction product of rhenium soluble oxide (Eq. 1.3) in polarography studies is difficult to explain and the information to support its existence is insufficient. It is noteworthy that the ΔG formation of Re^- is positive according to encyclopedias of electrode potentials [31]. This anion was not formed in aqueous solutions according to the experimental conditions reported by García [6], for this reason it is not considered in the diagram.

Table 2.1. Equations for the construction of the Figure 2.1 [1].

Reaction	Equation	Eq.
$2H^+ + 2e^- \rightarrow H_2$	$E = -0.059\,pH$	2.2
$Re^{3+} + 3e^- \rightarrow Re$	$E = 0.300 + 0.0197 \log a_{Re^{3+}}$	2.3
$ReO_4^- + 8H^+ + 7e^- \rightarrow Re + 4H_2O$	$E = 0.369 - 0.0675\,pH + 0.0084 \log a_{ReO_4^-}$	2.4
$ReO_2 + 4H^+ + 4e^- \rightarrow Re + 2H_2O$	$E=0.276-0.0591 pH$	2.5
$Re_2O_3 + 6H^+ + 6e^- \rightarrow 2Re + 3H_2O$	$E = 0.227 - 0.0591 pH$	2.6
$ReO_4^- + 8H^+ + 4e^- \rightarrow Re^{3+} + 4H_2O$	$E = -0.422 - 0.1182\,pH + 0.0148 \log \frac{[Re^{3+}]}{[ReO_4^-]}$	2.7
$2Re^{3+} + 3H_2O \rightarrow Re_2O_3 + 6H^+$	$\log(Re^{+++}) = -3.69 - 3pH$	2.8
$2ReO_2 + 2H^+ + 2e^- \rightarrow Re_2O_3 + H_2O$	$E = -0.375 - 0.0.0591 pH$	2.9
$ReO_3 + 2H^+ + 2e^- \rightarrow ReO_2 + H_2O$	$E = 0.399 - 0.0591\,pH$	2.10

The pH dependences of several reactions were calculated based on the Eq. 2.2 to 2.10 listed in Table 2.1. The reactions of metallic rhenium in Figure. 2.1a occurs at close potentials in the pH range of the experimental conditions in this study; except for Re^{3+}. On the other hand, the Figure. 2.1b, shows that Re^{3+} can easily evolve to ReO_4^-. Gómez et al [39] determined the voltammetry behavior of rhenium in acid dissolutions and postulated that the HER was convoluted with the cathodic current of the reaction (Eq. 1.3), which is the formation of rhenide anion. However, the upper limit of the voltammetry was superior to 0.4 V, possibly indicating the formation of rhenium oxides or Re^{3+}. Subsequently the current cannot be related directly with the Re^-. Predominance diagram in Figure. 2.1d is plotted to ensure that Re^{3+} can be expected in acid solution. This diagram displays that Re^{3+} is stable at high concentration of protons. For this reason, under the experimental conditions used in this work (pH= 0.3), the formation of the Re^{3+} ion was not expected. Subsequently, Re_2O_3 is the specie that is formed in the surface of electrode. It is important to mention that Re_2O_3 has been reported to decompose into hydrous ReO_2 and metallic Re [40-41], according to the following reaction (Eq. 2.12).

$$2Re_2O_3 + 6H_2O \rightarrow Re + 3(ReO_2 \cdot 2H_2O) \qquad \text{Eq. 2.11}$$

The Figure. 2.1c shows the immunity domain (formation of metallic Re), passivation domain (formation of Re_2O_3, ReO_2, ReO_3) and anodic corrosion domain (corresponding to the formation of ReO_4^-).

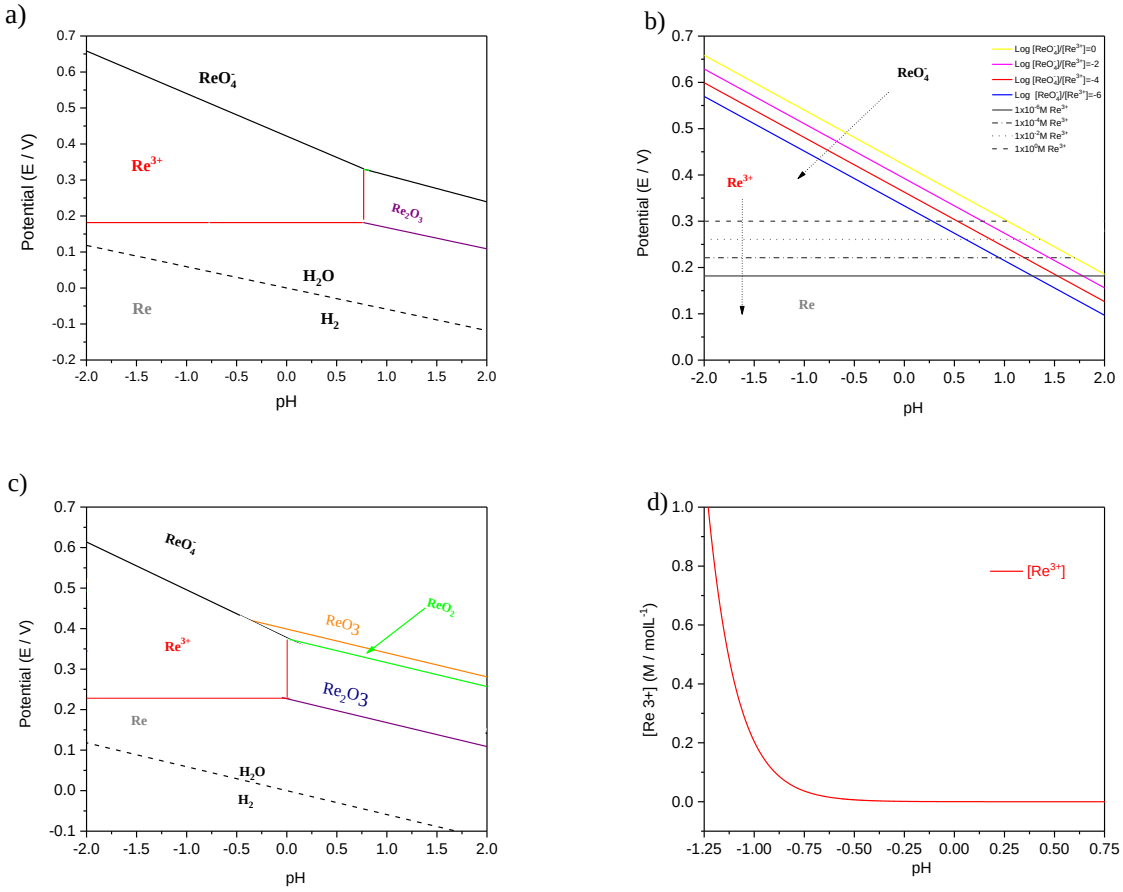

Figure 2.1. Potential-pH diagrams for rhenium a) potential dependences for Re/$Re^{3+}$and Re^{3+}/$Re\ O_4^-$ reactions at low potentials, b) potentials variation for Re, Re^{3+}, $Re\ O_4^-$ species at different concentrations (the direction of the arrows indicated changes from high to low concentration) c) corrosion diagram of rhenium and d) [Re^{3+} ion] vs pH.

2.3 Potential-pH diagram for methanol.

The electrooxidation of alcohols to carbon monoxide using platinum as electrocatalyst and their alloys had been extensively studied [42-57]. Consequently, the E-pH diagram of these species is shown in Figure. 2.2, according to the equations listed on Table 2.2 [58-59]. It is theoretically predicted that the methanol electrooxidation begins below 0.1 V vs SHE and this reaction could occur on metallic platinum. However, experimentally the reactivity does not occur below 0.1 V vs SHE. This implies that electrooxidation of methanol on platinum occurs at potentials without any technological application.

Table 2.2. Half-reactions and Nernst equations for the construction of the methanol and platinum E-pH diagram.

Reaction	Nernst Equation	Eq.
$Pt + 2H_2O \leftrightarrow Pt(OH)_2 + 2H^+ + 2e^-$	$E = 0.980 - 0.0591pH$	2.12
$Pt + 2H_2O \leftrightarrow Pt(OH)_2 + 2H^+ + 2e^-$	$E = 0.963 + 0.0295 \log[Pt^{2+}]$	2.13
$CO_2 + 6H^+ + 6e^- \leftrightarrow CH_3OH + H_2O$	$E = 0.015 - 0.0591pH$	2.14
$CH_3OH \leftrightarrow HCOH + 2e^- + 2H^+$	$E = 0.232 - 0.0591pH$	2.15*
$CH_3OH + H_2O \leftrightarrow HCO_2H + 4e^- + 4H^+$	$E = 0.145 - 0.0591pH$	2.16*
$CH_3OH + 2H_2O \leftrightarrow H_2CO_2H + 6e^- + 6H^+$	$E = 0.044 - 0.0591pH$	2.17*
$\frac{1}{2}O + 2H^+ + 2e^- \leftrightarrow 2H_2O$	$E = 1.23 - 0.0591pH$	2.18

*The species concentration was considered as$1x10^{-6}$ M.

According to the diagram in Fig. 2.2, it can be predicted that methanol does not influence the HER on platinum. However, in experiments it was observed that the adsorption of methanol blocked the HER on platinum. It is possible that the methanol could have been electro-oxidized to formic carbonic acid, formic acid and formaldehyde according with Fig. 2.2b. It is commonly accepted that the electrooxidation of methanol on platinum surfaces proceeds via a duel pathway mechanism; (direct pathway) reactive intermediates and (indirect pathway) poisoning intermediates as monoxide carbon [60].

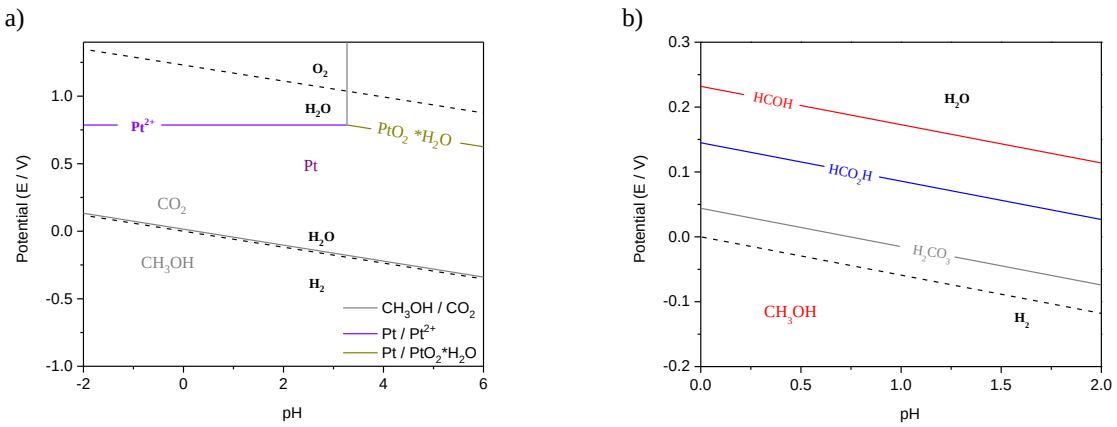

Figure 2.2. Pourbaix diagram of: a) methanol – platinum and b) methanol, lines represent the borders of thermodynamic stability of methanol, which can be electrooxidized to carbonic acid (—), formic acid (—) and formaldehyde (—). The dotted lines (**- - -**) indicates the stability of water at 298.15 K.

It has been shown that j_0 of the HER varies with the medium [34] on electrodeposited rhenium electrodes, however the influence of methanol in the HER on metallic rhenium has not been reported in literature. The competition for adsorption sites between the proton and methanol in several metals is well-established [42-43], but information of rhenium is not included. Some works reported the influence of methanol in the HER [42-44] for different electrodes and the differences in the adsorption process produce a variation on the methanol electrooxidation overpotential.

2.4 Behavior of log j_0 as a Function of Metal Substrate including Rhenium.

In Chapter 1, it was mentioned that several authors reported kinetic data of the seminal paper of Trasatti [61] as well as the tabulated by Appleby and Kita [62]. Trasatti [61] and Appleby and Kita [62] enlisted the exchange current densities for HER, for as many metals as possible. There are 29 exchange current densities of metals reported by both, Trasatti [61] and Appleby [62], the standard deviation (σ) of these data is included in the table 2.3. There is minor dispersion ($\sigma < 1.0$), for most of the data; except for silver (σ=3.5), antimony (σ=1.54), and rhenium (σ=1.4), which present the highest standard deviations. There are more than three orders of magnitude as difference between the worst and the best electrocatalytic activity. The criteria of reliable data exchange currents of polycrystalline and monocrystalline silver were introduced by Santos [63], but no information was provided for antimony and rhenium. The question is why these exchange currents values have not been reviewed before? A possible answer is that these metals

have low relevance in the development of hydrogen technology. In addition, it is even more important to clearly determine the electrocatalytic activity of the hydrogen evolution on single crystals, as one can see from the studies of Eberhardt [64] and Nakamura [65]. Trasatti [61], Appleby and Kita [62] found a periodicity of j_0, which is the main characteristic of the elements on the periodic table: all properties of elements change periodically, including the exchange current density for the HER. In recent times, the volcano curve had been rediscovered because a new data of adsorption energy of hydrogen on several metals had been calculated using the density functional theory, for example [66, 67]. There is a discussion if the estimation of Gibbs free energy of adsorption (ΔG) of the HER on the new volcanos plots reflects the proper values [68]. However, these new studies used the exchange currents reported by Pecherskaya (log j_0 =-3) [69] and not the data reported by Joncich (log j_0 =-5.1), see Table 2.3. [70]. The volcano plot reported by Schmickler and Trasatti [61,68] used j_0 as reported by Pecherskaya [69] in sulfuric acid. On the other hand, Appleby [62] used the data reported by Joncich [70], who studied the HER in acid chloride and sulfuric acid. There is a difference of three orders of magnitude between the data reported by Pecherskaya [69] and the one reported by Joncich [70].

Theoretical studies need to compare with reliable experimental data to produce a significant conclusion, but it conversely causes confusion. For example, Andreev [66] relates Hydrogen evolution overvoltage (η_{H_2}) with calculated surface energy (U_S) of several metals including the elements of the sixth period of the periodic table: Au (79), Pt (78), Ir (77), Os (76) Re (75), W (74) and Ta (73), see Figure 2.3 (this figure was plotted with Trasatti [61], Andreev [66] and Kopylets [71] values). Andreev [66] established a discussion about why the U_S presents a linear correlation with adsorbed hydrogen atom and consequently with the hydrogen overvoltage. Although, Andreev [66] observed a linear correlation with some metals, their figures do not display this correlation for the sixth period metals (Figure 2.3). It is noteworthy that the calculated overvoltage of HER on rhenium was not reported in the work of Andreev [66].

Table 2.3. Experimental values of exchange current reported by Trasatti [61] and Appleby [62], mean values between both and standard deviation.

Atomic number-element symbol	Log j_0 / A cm^{-2} [62]	Log j_0 / A cm^{-2} [61]	Log j_0 mean value / A cm^{-2}	σ
22 Ti	-6.9	-8.3	-7.6	0.990
23 V	-6.2	No data	-6.2	
24 Cr	-6.4	-7	-6.7	0.424
26 Fe	-5.8	-5.6	-5.7	0.141
27 Co	-4.9	-5.3	-5.1	0.283
28 Ni	-5.2	-5.25	-5.23	0.035
29 Cu	-7.4	-7.8	-7.6	0.283
30 Zn	-10.5	No data	-10.5	
40 Zr	-6.7	No data	-6.7	
41 Nb	-7.3	-8.4	-7.85	0.778
42 Mo	-6.5	-7.3	-6.9	0.566
44 Ru	-3.3	-4.2	-3.75	0.636
45 Rh	-2.5	-3.5	-3.0	0.707
46 Pd	-2.4	-3.1	-2.75	0.495
47 Ag	-6.4	-11	-8.7	3.253
48 Cd	-12	-11.6	-11.8	0.283
49 In	-10.9	-9.5	-10.2	0.990
50 Sn	-9.2	-7.8	-8.5	0.990
51 Sb	-8.7	-5.1	-6.9	2.546
73 Ta	-7.8	-8.5	-8.15	0.495
74 W	-6.4	-6.4	-6.4	0.000
75 Re	-5.1	-3.0	-4.05	1.485

(continued next page)

Table 2.3. continued…

Atomic number-element symbol	Log j_0 / A cm^{-2} [62]	Log j_0 / A cm^{-2} [61]	Log j_0 mean value / A cm^{-2}	σ
76 Os	-4.0	-4.1	-4.05	0.071
77 Ir	-3.3	-3.6	-3.45	0.212
78 Pt	-3.3	-3.1	-3.2	0.141
79 Au	-5.7	-6.5	-6.1	0.566
80 Hg	-11.9	-12.6	-12.25	0.495
81 Tl	-11.5	-10.53	-11.02	0.686
82 Pb	-12.6	-11.4	-12	0.849

The a was calculated with basis in the tafel slope (Eq. 2.19) and the parameter a, which combines the Tafel and j_0 (Eq. 2.21).

$$b = \frac{RT}{\alpha F} 2.303 \qquad \text{Eq. 2.19}$$

$$a = \frac{RT}{\alpha F} 2.303 \log j_0 \qquad \text{Eq. 2.20}$$

Where R is the universal gas constant, F is the well-known Faraday constant and, α is the symmetry factor.

Figure 2.3 displays the parameter a versus the calculated surface energy U_s by Andreev [66]. Then, questions emerge from this figure, if Ta, W and Re, have similar surface energy 147.72, 174.84 and 171. kJmol^{-1} respectively; so, why the performance of rhenium is the same than platinum with 97 kJmol^{-1} as surface energy? In addition, Pd possesses a low surface energy U_s (79.5 kJmol-1) lower than Re, also Pd follows the Andreev correlation for α-ΔU_s [66] (dotted line in Figure 2.3). However, both presented the same performance towards the HER. So, this work was additionally focused in finding some answers to this question.

Andreev [66] proposed that the enthalpy of the adsorption of hydrogen atoms ($\Delta H_{ad,H}$) is connected directly with the surface energy of a metal, equations (Eq. 2.22). Then the U_s

calculated by Andreev [66] can be compared with enthalpies obtained by a numerical simulation of metal clusters performance by Kopylets [71]. The enthalpies calculated by Andreev [66] or Kopylets [71] are quite different.

$$\Delta U_s = -\Delta H_{ad,H\cdot} \qquad \text{Eq. 2.21}$$

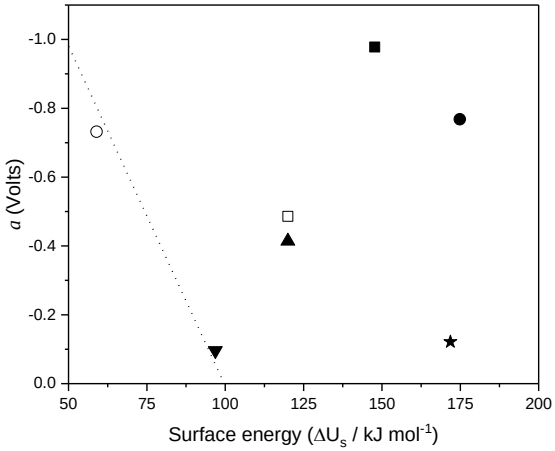

Figure 2.3. . Variation of the parameter *a* versus the surface energy. Ta (■), W (●), Re (★), Os (□), Ir (▲), Pt (▼), Au (○) and the Andreev [66] correlation for *a*-ΔU_s (dotted line). *a* values were calculated using data in Table 2.3 and Eq. 2.21. For Os, the enthalpy of the adsorption of hydrogen reported by Kopylets [71] was used instead of ΔU_s.

The adsorption energy of hydrogen of several metals calculated by Kopylets [71] and the exchange currents of HER on these metals varied periodically with the atomic number, see Figure 2.4. Before discussing this plot, there is one point that must be first clarified: in metals as gold, silver and copper the *d* orbitals do not play a role in the hydrogen bonding, these metals participate with *sp* orbitals [72]. Consequently, only metals with *d* orbitals were included in Figure 2.4. This plot displays that the metals of the four, five and sixth period of the periodic table do not strictly follow the trend imposed by the Sabatier principle. Particularly, the behavior of the elements of the sixth period shows an abrupt change between Os (76) and Re (75), this abrupt change can be due the discrepancy in the determinate j_0 value for Re, see the standard deviation in Table 2.3.

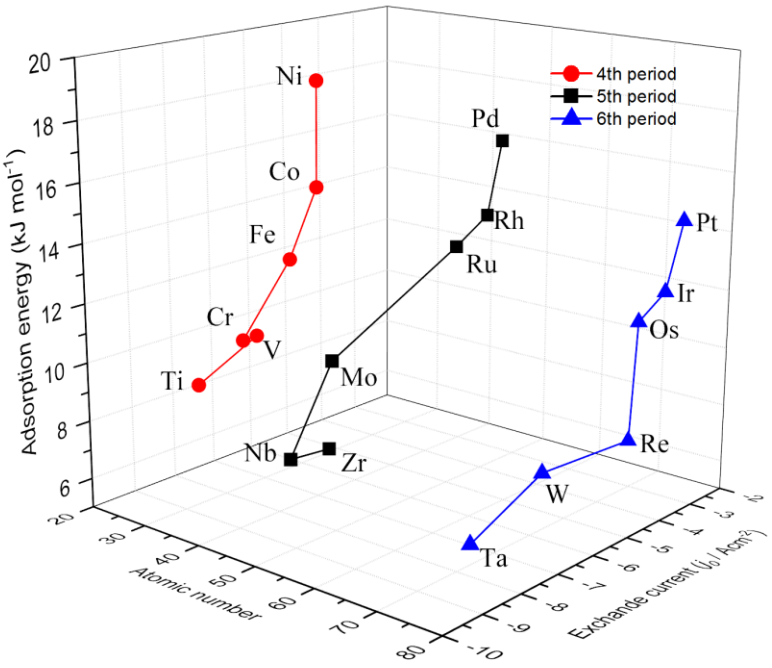

Figure 2.4. Energies of the hydrogen adsorption calculated by Kopylets [71] - mean values exchange currents densities (Table 2.3) - atomic number, plot.

Kita [73] found a periodic comportment when plotting the j_0 against the atomic number, similar to the Figure 2.4. To be clearer, the log j_0 increases at beginning of each *n*-th period, reaches a maximum value, then decreases quite sharply to a minimum value. The electroactivity towards HER increases firstly with the increment of atomic number, reaches the maximum with metals of the group VIII (Ni, Pd and Pt), decreases bluffly to the minimum for metals of the IB group (Cu, Ag, Au) and IIB (Zn, Cd Hg), and then increases again with further increase of the atomic number. A comparable periodicity has been observed with the hydrogen overvoltage of metals at a fixed electrical current density [62]. It is clear from Figure 2.4 that Re and Os cannot have the same current density, for this illogical behavior, it is necessary to understand or to find an explanation to realize this comportment.

It is postulated that the main factor that controls the reaction rate for individual rate-steps on diverse metals is the heat of adsorption of hydrogen, and then log j_0 can be correlated with this heat. However, it is hard to find a trend between these two properties in the case of Re, because this metal is distinguished by their isolation. In Figure 2.5a the experimental heats of adsorption of hydrogen on metals decrease from the beginning to the end of a row in the periodic table, except for Ti. Then, the heats increase as the *d*-

shell is filled with electrons in 6-th period (Pt (78), Ir (77), Os (76) Re (75), W (74) and Ta (73)). At this point, it is important to recall that the *d*-orbitals are responsible for the hydrogen adsorptive characteristics, while the *s*- and *p*- electrons are decisive for electrical conductivity. If the adsorption involves bonding with available atomic orbitals within the metal, then the strength of the bond should increase with the number of empty *d*-orbitals [75].

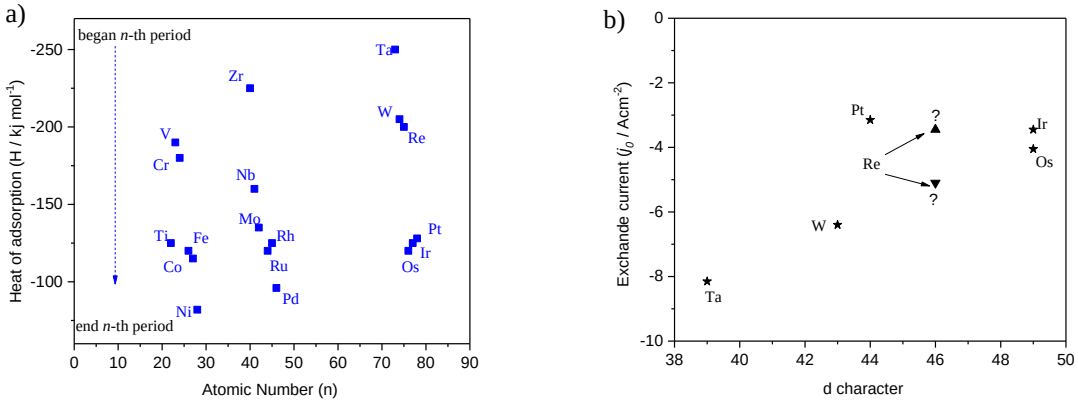

Figure 2.5. a) The variation of experimental heats of adsorption of hydrogen from [71] on metals as a function of atomic number; b) the mean value exchange currents densities of several metals (Table 2.3) versus *d* character [75].

The number of paired electrons is quantified by means of *d*-character, and the higher the percentage *d*-character of the metal the fewer *d*-orbitals are available to adsorbate bonding. Also, it is expected that metals with more unpaired electrons (vacancies in the *d*-orbitals), interact with hydrogen atoms adsorbing them very strongly [76]. In Figure 2.5b, the lower the percentage of the *d*-character of Ta (73), the higher adsorption of hydrogen atoms, which implies a difficult desorption of atoms, resulting in high experimental heat of adsorption of hydrogen and a slower reaction rate of the HER. In Figure 2.5b, Pt (78) has an intermediate value of the *d*-character, which leads to a decrease of adsorption bonding (lower heat of adsorption), and to an increment of the reaction rate of HER. Thus, properties like the *d* character can determine the heat of adsorption and the log j_0 value of hydrogen. Figure 2.5b shows two different data reported for HER on Re and at least two controversial conclusions can be obtained from this figure. Several correlations for the variation of the j_0 of the HER with (a) metal-hydrogen bond strength, (b) percentage *d*-character, and work function (c) have been explored during the twentieth century. In section 1.3 it was mentioned that the studies reported by Bockris and Conway [77] as well as Harinipriya and Sangaranarayanan [78] introduced a direct

link between the j_0 and the work for several metals. These authors [78] postulated an explicit expression for the exchange current density for HER incorporating the work function of metal electrode (Φ_M) and desolvation free energy of the reactant, see equation Eq. 2.22. The central idea of these authors is that the k_{et} electron transfer rate constant is directly related to the exchange current density j_0.

$$j_0 = f(k_{et}, \exp \Delta G_{H^+-S}) \qquad \text{Eq. 2.22}$$

$$k_{et} = (k_b T / h) \exp\left(-\frac{\Delta G^{\neq}}{RT}\right) \qquad \text{Eq. 2.23}$$

Furthermore, in Eq. 2.23 k_{et} is a function of the free energy of activation ($\Delta G^{\neq}$) and temperature, where k_b and h are the Boltzmann and Planck constant, respectively. $\Delta G^{\neq}$ depends on three elements in the equation Eq. 2.24: 1) the transference of electrons from the metal to the reactant, 2) the work (w_r) done when bringing the reactant from bulk to the reaction zone and 3) the work (w_p) done to send the product from the reaction zone to bulk. These works comprise the desolvation energy (ΔG^{inter}) and are also determined by the surface potential χ, see Eq. 2.25.

$$\Delta \mathrm{G}^{\neq} = \frac{(\mathrm{w_r} + \mathrm{w_p})}{2} + \Delta \mathrm{G_{et}} \qquad \text{Eq. 2.24}$$

$$\mathrm{w_r} + \mathrm{w_p} = \mathrm{w} = \Delta \mathrm{G}^{inter} - \mathrm{zF}\chi \qquad \text{Eq. 2.25}$$

Where z denotes the charge of the reactant or product and F is again Faraday constant. Other key idea is that, the work function of the solvated electrode is the difference between the work function of the metal and the solvation free energy of electrons in solution. Then, it can be postulated that the Gibbs free energy change is function of Φ_M, Eq. 2.26.

$$\Delta G_{et} = f(S, \chi, \Phi_M) \qquad \text{Eq. 2.26}$$

Eq 2.28 is obtained by combining Eq 2,23 and Eq 2.27:

$$j_0 = \left(\frac{FC_{H+}k_bT}{Ah} \right) \exp\left(-\frac{\Delta G_{H^+-S}}{2S_{N_{H^+}}RT} - \frac{z_{H^+}Fx_e^s}{2RT} + \frac{F\xi\Phi_M}{RT} \right)$$ Eq. 2.27

Where:

j_0 = exchange current density for HER on the metal

F = 96 485.3365 s A mol-1; Faraday constant,

$C_{H+} = 1M$ or $C_{H+} = 0.5M$, Molar concentration of ion H^+ represented in moles

k_b = 1.3806488 × 10^{-23} m^2 kg s^{-2} K^{-1}; Boltzmann constant,

T = 298 K; Absolute temperature,

A = 0.001 cm^{-2} the electrode area

h = 6.62606957 × 10^{-34} m^2 kg s^{-1}; Planck constant,

R = 8.3144621 J K^{-1} mol^{-1}; Universal gas constant,

ΔG_{H^+-S} = 11.98 eV; Desolvation free energy of the reactants

$S_{N_{H^+}}$ = 5; Solvation number of protons

z_{H^+} = 1; Charge of H^+

x_e^s =-0.4 eV, Surface potential

ξ = 0.17, Dimensionless constant,

Φ_M = is the work function of the metal

The Eq 2.27 is related to the j_0 for HER, the work functions [79-81] and desolvation energy of the reactants. When the fundamental constants and variables are used appropriately in equation (Eq 2.27), j_0 can be calculated. However, the j_0 of HER on metallic Re (Table 2.4) and Pt (Table 2.5) were estimated based on the metal work function reported in the literature. In Figure 2.6, the three coinage metals (Au, Ag, Cu) show a regular performance for HER, because the position of their *d* bands are unfavorable for the hydrogen adsorption (Figure 2.6).

Table 2.4. Estimation of Exchange Current Density for HER on rhenium using Equation 2.2, considering 0.001 cm^2 as electrode Area.

Φ (eV)	Concentration on surface (mol cm^{-2})	Calculated -log j_0 /A cm^{-2}	σ respect -log j_0=6.0	Reference of the work function value
4.72	7.5 $HClO_4$	5.494	0.358	[78]
4.72	0.5 M H_2SO_4	6.370	0.261	[78]
4.82	7.5 M H_2SO_4	5.207	0.560	[80]
4.82	0.5 M H_2SO_4	6.083	0.058	[80]
4.87	7.5 $HClO_4$	5.064	0.662	[80]
4.87	0.5 M H_2SO_4	5.939	0.043	[80]
4.95	7.5 $HClO_4$	4.835	0.824	[78]
4.95	0.5 M H_2SO_4	5.710	0.205	[78]
4.96	7.5 $HClO_4$	4.806	0.844	[79]
4.96	0.5 M H_2SO_4	5.681	0.225	[79]
5.10	7.5 $HClO_4$	4.405	1.128	[79]
5.10	0.5M H_2SO_4	5.280	0.509	[79]
5.50	7.5 $HClO_4$	3.258	1.939	[79]
5.50	0.5M H_2SO_4	4.133	1.320	[78]
5.75	7.5 $HClO_4$	2.541	2.445	Re (1011) [80].
5.75	0.5M H_2SO_4	3.417	1.826	Re (1011) [80].

Table 2.5. Estimation of exchange current density for HER on platinum using Equation. Area of 0.001cm^2.

Φ (eV)	Concentration on surface (mol cm^{-2})	Calculated - Log j_0 (A cm^{-2})	Reference of the work function value
5.03	0.5 M H_2SO_4	5.48	[61]
5.64	0.5 M H_2SO_4	3.73	[78]
5.03	5 M H_2SO_4	4.48	[51]
5.64	5 M H_2SO_4	2.73	[78]

In Table 2.5, the values estimates for j_0 from the work function value correspond to the j_0 plotted on the volcano plot. Then platinum, iridium, osmium, rhenium, tungsten and tantalum were exclusively included in Figure. 2.6. This plot was constructed with *selected values* of Φ-coordinate and log j_0-coordinate. As can be expected for the selection of log j_0-coordinate were used experimental values of log j_0 enlisted in Table 2.3. Then, several key points emerged from this figure:

1. Ta (73) The Φ-coordinate and log j_0-coordinate are (4.23 eV, -8.15)
2. W (74) The coordinates are (4.55 eV, -6.4)
3. Re (75) There are several values of the work function reported in literature [79-81], but the majority are in the range 4.72 eV to 5.10 eV, except for Re monocrystal 5.75 eV[78] this value out of range was used to justify a high performance of metallic Re (log j_0 = -3.26) reported by Pecherskaya (log j_0 =-3) [69]. There is uncertainty in both coordinates. It is important to mention that the polycrystalline rhenium work function value is not greater than 5.0 eV, that is, lower than the single-crystal surfaces. Then, the average value work function observed by Wilson [79] is 4.96 ± 0.5 eV for polycrystalline rhenium. This average is a reference for the future selection of Φ-coordinate. Chapter 3 will focus on the establishment of a log j_0-coordinate, which will enhance data quality.
4. Os (76) The range of variation of the calculated log j_0 can reach more than 3 orders of magnitude. The exceptionally high melting point of Os indicates that it cannot be easily purified. Arblaster [82] commented that the properties values of Os were determined on impure metal and using 1960s technology for the measurements. Kawano [81] collects hundreds of work functions measurement for all metals and found a decided discrepancy (1.1 eV) between data reported for Os. We interpret that there is some

uncertainty in determining the work function of this metal, but the log j_0 is straightforward to identify. This value reduce uncertainty and it can be postulated the coordinates on the figure (5.24 eV,-4.05).

5. Ir (77) There is some uncertainty of the data, however the rate of HER on Ir is faster and then it can be postulated that the coordinates are (5.3 eV, -3.71)
6. Pt (78) There is some vagueness of the data, nonetheless the faster rate of HER on Pt allows to postulate the coordinates (5.64 eV, -2.73).

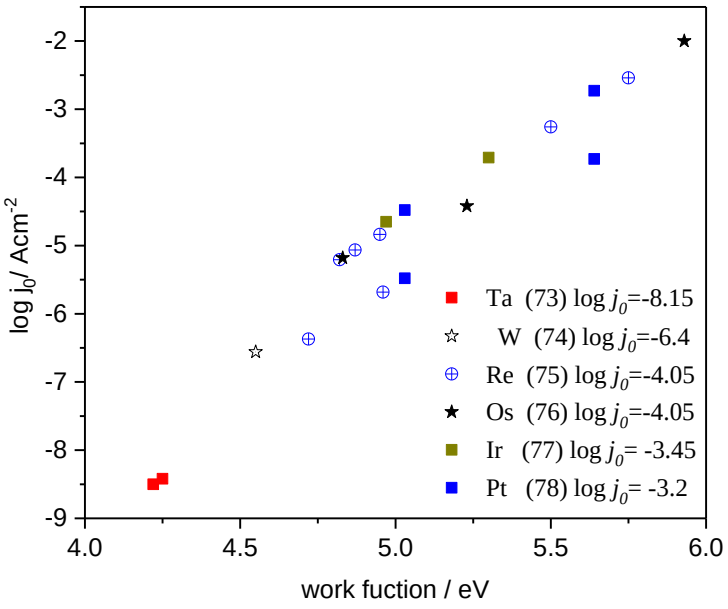

Figure 2.6. The plot of several Φ-coordinate versus log j_0-coordinate with based on Table 2.4 and 2.5 data.

In Table 2.4 the electronic structure of polycrystalline rhenium was incorporated via their work function and the results predicted that the kinetics of heterogeneous electron-transfer reactions on polycrystalline rhenium is slower than the single-crystal surfaces of rhenium (1011).

In 1957, Bockris and Conway [77] established a linear relation between log j_0 values and the metal work functions and in 1972 Trasatti [61] determinated this linear correlation in Eq 2.28.

$$\log j_0 = 6.7\Phi_M - 36.6 \text{ (Eq 2.29)} \qquad \text{Eq. 2.28}$$

It is important to mention that for Eq 2.28, is possible use different values of Φ, however, a plot with estimated values of j_0 will be compared with the one constructed with the experimental presented on chapter III.

Metallic rhenium (fused) is made using powder metallurgical techniques or it can be made by arc melting in an inert atmosphere [83]. This study is focused in analyzing the HER on rhenium obtained by a metallurgical process, however there are several studies of HER on rhenium electrodeposited, this is known as rhenized surfaces [37,84-91], as example, Muñoz [87] studied the photoelectrocatalytic effect in the HER by the rhenium electrodeposition process on p-Si(100).. Méndez [84] commented that the electrocatalytic activity of the rhenized surfaces towards the HER had controversial points. In these studies, after the electrodeposition of soluble oxides of rhenium, the oxygen-containing impurities were reduced in saturated solutions with gaseous hydrogen. Krasikov [34] commented that the processes do not remove completely the oxygen, as a result the rhenium obtained impurities which formed rhenium-hydrogen bronzes H_xReO_y [92] or ReH_2 [93] which are difficult to electrochemically reduce to metal. In this regard, Zerbino [86] reported that in the electrodeposition of ReO_4^{2-} there was a formation of film with metallic Re containing H_2 occluded. For the latter, the comparison between different HER of rhenized surfaces and on metallurgical rhenium will be done in future studies.

2.5 Predicted mechanics of methanol electrooxidation on Rhenium by theoretical methods.

Cathro [94] commented the performance of metallic rhenium and their alloys towards the electrooxidation of methanol on metallic rhenium. However, it is not clear which is the performance of metallic rhenium. On the other hand, in the theoretical study reported by Ferrin [95] the performances of rhenium and ruthenium are similar. In the first instance, it is expected that rhenium and ruthenium are the most active in the de-hydrogenation of water. Ferrin et al. [95] investigated the reaction mechanics of electrooxidation of methanol on 12 metals, including rhenium, using density functional theory (DFT). These authors estimated the adsorption free energies of various intermediates with basis in two key descriptors for each metal surface: the free energies of OH^- and CO on the surface. The lack of experimental data of the methanol electrooxidation on metallic rhenium motivates the present study.

The Figure 2.7 was constructed with the data reported by Ferrin et al. [95] and their calculations predict the mechanism of the methanol electrooxidation on rhenium, this follows a pathway with monoxide carbon as intermediary, see Eq. 2.290 to 2.34. It is expected to compare the experimental results with DFT calculations performance by Ferrin [95]. On the other hand, Garcia [96] studied the HER on polycrystalline rhenium using electrochemical impedance spectroscopy (EIS). His results suggested that the Randles circuit describe the HER on rhenium, to complete the study it is necessary to make experiments in presence of methanol, therefore motivating the present study.

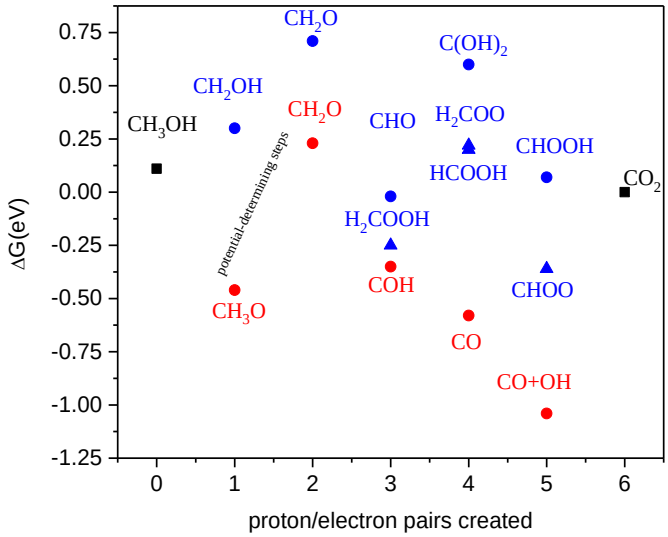

Figure 2.7. Free energies for the intermediates of methanol electro-oxidation on rhenium [95]. Red symbols are the most stable. The symbols in black correspond to methanol and the CO_2. The x-axis indicates how many proton/electron pairs have been created from the original methanol.

$$CH_3OH \rightarrow CH_3O_{(ads)} + H^+ + e^- \quad \text{(Eq. 2.29)}$$

$$CH_3O_{(ads)} \rightarrow CH_2O_{(ads)} + H^+ + e^- \quad \text{(Eq. 2.30)}$$

$$CH_2O_{(ads)} \rightarrow COH_{(ads)} + H^+ + e^- \quad \text{(Eq. 2.31)}$$

$$COH_{(ads)} \rightarrow CO_{(ads)} + H^+ + e^- \quad \text{(Eq. 2.32)}$$

$$H_2O_{(l)} \rightarrow OH_{(ads)} + H^+ + e^- \quad \text{(Eq. 2.33)}$$

$$CO_{(ads)} + OH_{(ads)} \rightarrow CO_{2(g)} + H^+ + e^- \quad \text{(Eq. 2.34)}$$

2.6 References.

[1] Pourbaix M. Atlas of Electrochemical Equilibrium in Aqueous Solutions. 2nd ed. TEXAS: National Association of Corrosion Engineers Houston; 1974.

[2] Magee RJ, Cardwell T. Encyclopedia of Electrochemistry of the Elements. Vol.2. New York: Marcel Dekker, New York; 1973.

[3] Giraudeau A, Lemoine P, Gross M. Electrochemical oxidation of rhenium. Corros Sci 1973; 13:421–32.

[4] Darab JG, Smith PA. Chemistry of technetium and rhenium species during low-level radioactive waste vitrification. Chem Mater 1996; 8:1004–21.

[5] Takeno N. Atlas of Eh-pH diagrams. Geol Surv Japan Open File Rep 2005; 419:102.

[6] Garcia-Garcia R, Ortega-Zarzosa G, Rincón ME, Orozco G. The Hydrogen Evolution Reaction on Rhenium Metallic Electrodes: A Selected Review and New Experimental Evidence. Electrocatalysis 2015; 6:263–73.

[7] Srivastava RR, Lee J chun, Kim M seuk. Complexation chemistry in liquid-liquid extraction of rhenium. J Chem Technol Biotechnol 2015; 90:1752–64.

[8] Zhulikov V V., Gamburg YD. Electrodeposition of rhenium and its alloys. Russ J Electrochem 2016; 52:847–57.

[9] Kanamura S, Mizuguchi K, Fujita R, Kondo N. Electrodeposition of Rhenium Species at a Stainless Steel Electrode from Acidic, Neutral, and Alkaline Solutions 2014;161:92–6.

[10] Shaldaev VS, Malofeeva AN, Davydov AD. Determination of corrosion rate of molybdenum, rhenium and their alloys in sodium chloride solution by the method of Tafel extrapolation. Russ J Electrochem 2014; 50:994–8.

[11] Davydov AD, Shaldaeva VS, Malofeevaa AN, Chernyshovab O V, Volgina VM. Determination of Corrosion Rate of Rhenium and Its Alloys. Chem Eng 2014;41.

[13] Lingane, J. J. Polarographic Investigation of Rhenium Compounds. I. Reduction of Perrhenate Ion at the Dropping Mercury Electrode. Journal of the American Chemical Society, 64 (1942) 1001-1007.

[13] Lingane, James J., Polarographic Investigation of Rhenium Compounds. II. Oxidation of—1 Rhenium at the Dropping Electrode and the Potential of the Re^{+2}—Re^{-1} Couple. Journal of the American Chemical Society 64 (1942) 2182-2190.

[14] Rulfs, Charles L., and Philip J. Elving, Oxidation Levels of Rhenium. I. Polarographic and Coulometric Reduction of Perrhenate, Journal of the American Chemical Society 73 (1951): 3284-3286.

[15] Rulfs, Charles L., and Philip J. Elving, Oxidation Levels of Rhenium. II. Oxidation of Rhenide at the Dropping Mercury Electrode. Nature of the Rhenide Species in Hydrohalic Acid Media, Journal of the American Chemical Society 73 (1951): 3287-3292.

[16] Hindman, J. C., & Wehner, P. Electrolytic Reduction of Perrhenate. I. Studies in Perchloric, Ethanesulfonic, Trifluoroacetic and Hydrochloric Acids. Journal of the American Chemical Society, 75 (1953) 2869-2872.

[17] Wehner, P., & Hindman, J. C. Electrolytic Reduction of Perrhenate. II. Studies in Sulfuric Acid. Journal of the American Chemical Society, 75 (1953) 2873-2877.

[18] Smith Jr, Wm T., J. W. Cobble, and G. E. Boyd, Thermodynamic Properties of Technetium and Rhenium Compounds. I. Vapor Pressures of Technetium Heptoxide, Pertechnic Acid and Aqueous Solutions of Pertechnic Acid, Journal of the American Chemical Society 75 (1953) 5773-5776.

[19] Cobble, J. W., Wm T. Smith Jr, and G. E. Boyd, Thermodynamic Properties of Technetium and Rhenium Compounds. II. Heats of Formation of Technetium Heptoxide and Pertechnic Acid, Potential of the Technetium-(IV)-Technetium (VII) Couple, and a Potential Diagram for Technetium, Journal of the American Chemical Society 75 (1953) 5777-5782.

[20] G. E. Boyd, J. W. Cobble, and Wm. T. Smith Jr., Thermodynamic properties of technetium and rhenium compounds. III. Heats of formation of rhenium heptoxide and trioxide, and a revised potential diagram for rhenium, J. Amer. Chem. Soc. 75 (1953) 5783-4.

[21] Smith Jr, Wm T., G. D. Oliver, and J. W. Cobble, Thermodynamic Properties of Technetium and Rhenium Compounds. IV. Low Temperature Heat Capacity and Thermodynamics of Rhenium, Journal of the American Chemical Society 75 (1953) 5785-5786.

[22] Cobble, J. W., G. D. Oliver, and Wm. T. Smith, Thermodynamic Properties of Technetium and Rhenium Compounds. V. Low Temperature Heat Capacity and the Thermodynamics of Potassium Perrhenate and the Perrhenate Ion, Journal of the American Chemical Society 75 (1953) 5786-5787.

[23] King, J. P., J. W. Cobble, Thermodynamic Properties of Technetium and Rhenium Compounds. VI. The Potential of the ReO3/ReO4-Electrode and the Thermodynamics of Rhenium Trioxide, Journal of the American Chemical Society 79 (1957) 1559-1563.

[24] Cobble J. W. On the structure of the rhenide ion. J. Phys. Chem. 61, 727 (1957).

[25] King, J. P., and J. W. Cobble, The Thermodynamic Properties of Technetium and Rhenium Compounds. VII. Heats of Formation of Rhenium Trichloride and Rhenium Tribromide. Free Energies and Entropies, Journal of the American Chemical Society 82 (1960) 2111-2113.

[26] Ginsberg, A. P.; Koubek, E. On the Nature of Lundel and Knowles Rhenide Ion. Z. Anorg. Allg. Chem. 1962, 315, 278−282 Ginsberg, A. P., & Koubek, E. (1962).

[27] Shropshire, J. A. (1968). Electrochemical reduction of perrhenate in sulfuric acid solution. Journal of Electroanalytical Chemistry and Interfacial Electrochemistry, 16(2), 275-278.

[29] Kohlíčková, M., Jedináková-Křížová, V., & Horejš, M., Influence of technetium and rhenium speciation on their sorption on natural sorbents. Czechoslovak journal of physics, 49 (1999) 695-700.

[30] M.S. Antelman, Encyclopedia of Chemical Electrode Potentials (Plenum Press, New York, 1982), p. 176

[31] A.J. Bard, R. Parsons, J. Jordan, Standard Potentials in Aqueous Solution (Marcel Dekker, New York, 1985), pp. 444–451.

[32] G. Inzelt, in The Encyclopedia of Electrochemistry Vol. 7, ed. A. J. Bard, M. Stratman, F. Scholz, C. J. Pickett, (Wiley-VCH, Weinheim, 2006), p. 35-36.

[33] S.G. Bratsch, Standard Electrode Potentials and Temperature Coefficients in Water at 298. J. Phys. Chem. Ref. Data 18, 1 (1989)

[34] Vladimir L. Krasikov. A new Approach to Mechanics of Hydrogen Evolution Reaction on Rhenium: 3D-Recombination, Bull Saint Petersbg State Inst Technol Technical Univ 2016;60:24–32.

[35] Li C, Agarwal J, Schaefer HF. The remarkable [ReH9]2- dianion: Molecular structure and vibrational frequencies. J Phys Chem B 2014; 118:6482–90.

[36] Ellis JE. Adventures with substances containing metals in negative oxidation states. Inorg Chem 2006; 45:3167–86.

[37] R. Schrebler, T, P. Cury, C. Suárez, E. Muñoz, F. Vera , R. Córdova, H. Gómez, J.R. Ramos-Barrado, D. Leinen, E.A. Dalchiele, Study of the electrodeposition of rhenium thin films by electrochemical quartz microbalance and X-ray photoelectron spectroscopy, Thin Solid Films 483 (2005) 50– 59.

[38] Vargas-Uscategui A, Mosquera E, López-Encarnación JM, Chornik B, Katiyar RS, Cifuentes L. Characterization of rhenium compounds obtained by electrochemical synthesis after aging process. J Solid State Chem 2014; 220:17–21.

[39] Gómez J, Gardiazábal JI, Schrebler R, Gómez H, Córdova R. Electrochemical behaviour of rhenium in aqueous solution, J Electroanal Chem 260 (1989) 113-126.

[40] Neil R. Murphy, Regina C. Gallagher, Lirong Sun, John G. Jones, John T. Grant, Optical and chemical properties of mixed-valent rhenium oxide films synthesized by reactive DC magnetron sputtering, Optical Materials 45 (2015) 191–196.

[41] Hahn BP, May RA, Stevenson KJ. Electrochemical Deposition and Characterization of Mixed-Valent Rhenium Oxide Films Prepared from a Perrhenate Solution: Langmuir; 2007, 23(21) 10837-10845.

[42] T. Iwasita, in: H. Gerischer, C. Tobias (Eds.), Advances in Electrochemical Science and Engineering, vol. 1, Verlag Chemie, 1990, p. 127.

[43] Rosy A. Lampitt, Linda P.L. Carrette, Martin P. Hogarth, Andrea E. Russell, In situ and model EXAFS studies of electrocatalysts for methanol oxidation, Journal of Electroanalytical Chemistry 460 (1999) 80–87.

[44] S. Wasmus, A. Küver, Methanol oxidation and direct methanol fuel cells: a selective review, Journal of Electroanalytical Chemistry 461 (1999) 14–31.

[45] a) T. Iwasita, Electrocatalysis of methanol oxidation, Electrochim. Acta, 2002, 47(22–23), 3663–3674; b) T. Iwasita, Erratum to Electrocatalysis of methanol oxidation [Electrochimica Acta 47(22–23):3663–3674], Electrochim. Acta, 2002, 48(3), 289–289.

[46] J. Poppe, Spektroelektrochemische Untersuchungen der Elektrooxidation von Methanol, Ethanol und Ethylenglykol in alkalischer Lösung an kalt-abgeschiedenen Mehrkomponentenschichtelektroden. Chemnitz, Techn. Universiẗat, Thesis Diss., 2001. Pages 12,23.

[47] B. Hoyos, El mecanismo de la electrooxidación de metanol y etanol una revisión bibliográfica, Dyna 69 (2002)9-22.

[48] Sánchez, C., González, J. y Hoyos, B. Desarrollo de catalizadores anódicos para celdas de combustible directas de etanol, propano y metano. IV Conferencia internacional de energía renovable, ahorro de energía y educación energética. Varadero, Cuba, 2005.

[49] F. H. Barros de Lima, Desenvolvimento de eletrocatalisadores dispersos para o cátodo de células a combustível alcalinas, Thesis Diss., (2006), pp 93.

[50] V. Del Colle, Estudos eletroquímicos e espectroscópicos da eletrooxidação de etanol, acetaldeído e ácido acético sobre Pt (110) modificada superficialmente por ósmio [thesis]. São Carlos, Instituto de Química de São Carlos; 2006 Pages 3, 25.

[51] B. Hoyos, C. Sánchez, J. González, J. González, Catalizadores anódicos basados en platino para celdas de combustible de etanol, Dyna 74 (2007) 195-202.

[52] B. Hoyos, N. Munera, F. Chejne, Tolerancia al CO en Celdas de combustible, Dyna 75 (2008) 123-136.

[53] Z. D. Mojović, Alumosilikati sa ugrađenim klasterima metala prelaznih grupa lb i lVb-Vlll kao elektrokatalitički materijali. Univerzitet u Beogradu, Thesis Diss., (2009) Page 121.

[54] M. A. Bavio, Estudio de materiales de electrodo para la detección de contaminantes ambientales, Universidad Nacional de La Plata, Thesis Diss. (2011) Pages 146-159.

[55] D. H. Duan, Z. L. Zhang, T. Zhang, S. B, Liu, X. G. Hao; Y. B. Li, Performance of Pt Ru/C Catalysts Doped with W, Ni and Sn for Electrocatalytic Oxidation of Methanol in Alkaline Media,. Chemical Journal of Chinese Universities-Chinese 11 (2011) 2618-2625.

[56] E. Telli, Nikel Çinko Kaplı Grafit Elektrotun Metanol Oksidasyonuna Katalitik Etkisinin Araştırılması", Çukurova Üniversitesi, Thesis Diss. (2011) Page 93.

[57] Dabo, Ismaila, Resilience of gas-phase anharmonicity in the vibrational response of adsorbed carbon monoxide and breakdown under electrical conditions, arXiv.org, e-Print Archive, Condensed Matter (2012), 1-11.

[58] J. Van Muylder, M. Pourbaix, Carbon, N. de Zoubov,M. Pourbaix, in Atlas of Electrochemical Equilibria in Aqueous Solutions (NACE, Texas, 1974), pp. 449-457.

[59] J. Van Murylder, N. de Zoubov and M. Pourbaix, Platinum, in Atlas of Electrochemical Equilibria in Aqueous Solutions (NACE, Texas, 1974), pp. 378–383.

[60] Angel Cuesta, Towards a Molecular Level Understanding of Electrochemical Interfaces and Electrocatalytic Reactions, Johnson Matthey Technol. Rev., 2014, 58, (4), 202–204.

[61] S. Trasatti, Work function, electronegativity, and electrochemical behavior of metals: III. Electrolytic hydrogen evolution in acid solutions, J. Electroanal. Chem., 39 (1972) 163.

[62] A. J. Appleby, H. Kita, M. Chemla, G. Bronoel, in Encyclopedia of Electrochemistry of the Elements Vol. 9, ed. A. J. Bard, (M. Dekker; New York, 1982), pp. 415, 456-457, 460-461, 489.

[63] Santos, E.; Quaino, P.; Schmickler, W. Theory of electrocatalysis: hydrogen evolution and more. Phys. Chem. Chem. Phys., 14 (2012) 11224-11233.

[64] Eberhardt, E. Santos, W. Schmickler, Hydrogen evolution on silver single crystal electrodes-first results, Journal of Electroanalytical Chemistry, vol. 461, no. 1-2, pp. 76-79, 1999.

[65] Masashi Nakamura, Toshiki Kobayashi, Nagahiro Hoshi, Structural dependence of intermediate species for the hydrogen evolution reaction on single crystal electrodes of Pt, Surface Science 605 (2011) 1462–1465.

[66] Y. Y. Andreev, Energy Profile of Hydrogen Evolution on Metals with Consideration of Their Surface Energy, Prot. Met. Phys. Chem. Surf., 48, 290 (2012).

[67] a) J. K. Nørskov, T. Bligaard, A. Logadottir, J. R. Kitchin, J. G. Chen, S. Pandelov, U. Stimming, Trends in the Exchange Current for Hydrogen Evolution. J Electrochem Soc 2005;152:J23; b) Nørskov J.K., Bligaard, A. Logadottir, Kitchin J.R., Chen J.G., Pandelov S., Stimming U., Response to “Comment on ‘Trends in the Exchange Currentfor Hydrogen Evolution” [J. Electrochem. Soc., 152, J23(2005)] J. Electrochem. Soc., 2006;153:L33-L33.

[68] W. Schmickler and S. Trasatti, Comment on “Trends in the Exchange Current for Hydrogen Evolution” [J. Electrochem. Soc., 152, J23 (2005)] J. Electrochem. Soc., 153 (2006) L31.

[69] Pecherskaya AG, Stender V V. Potentials of the evolution of hydrogen in acid solutions. Zhurnal Fiz Khimii 1950;24:856–9.

[70] Joncich MJ, Stewart LS, Posey FA. Hydrogen Overvoltage on Rhenium and Niobium Electrodes. J Electrochem Soc 1965;112:717. doi:10.1149/1.2423674.

[71] V. I. Kopylets, Heats of adsorption of hydrogen on metals, Materials Science 35, 438 (1999).

[72] Paola Quaino, Fernanda Juarez, Elizabeth Santos, Wolfgang Schmickler Beilstein, Volcano plots in hydrogen electrocatalysis – uses and abuses, J. Nanotechnol. 2014, 5, 846–854.

[73] H. Kita, Periodic variation ef exchange current density of hydrogen electrode reaction with atomic number, J. Res. Inst. Catal., Hokkaido Univ., 15 (1967) 35

[75] Gundry, P. M., & Tompkins, F. C. (1960). Chemisorption of gases on metals. Quarterly Reviews, Chemical Society, 14(3), 257-291.

[76] Paunović, P., Popovski, O., & Dimitrov, A. T. (2011). Hydrogen Economy: The Role of Nano-scaled Support Material for Electrocatalysts Aimed for Water Electrolysis. In Nanotechnological Basis for Advanced Sensors (pp. 545-563). Springer Netherlands.

[77] Conway BE, Bockris JO. Electrolytic Hydrogen Evolution Kinetics and Its Relation to the Electronic and Adsorptive Properties of the Metal. J Chem Phys 1957; 26:532.

[78] Harinipriya S, Sangaranarayanan M V. Influence of the Work Function on Electron Transfer Processes at Metals: Application to the Hydrogen Evolution Reaction. Langmuir 2002; 18:5572–8.

[79] Wilson RG. Vacuum thermionic work functions of polycrystalline Nb, Mo, Ta, W, Re, Os, and Ir. J Appl Phys 1966; 37:3170–2.

[80] Halas S. 100 Years of Work Function. Mater Sci 2006; 24:20–31.

[81] H. Kawano, Effective work functions for ionic and electronic emissions from mono- and polycrystalline surfaces Prog. Surf. Sci., 83 (2008), p. 1-165.

[82] J. W. Arblaster, What is the True Melting Point of Osmium? Platinum Metals Rev. 49 (2005) 166–168.

[83] Neikov, Oleg D. Naboychenko, Stanislav S. Murashova, Irina V. Gopienko, Victor G. Frishberg, Irina V. Lotsko, Dina V. (2009). Handbook of Non-Ferrous Metal Powders - Technologies and Applications. Elsevier. Page 480.

[84] E. Méndez M. F. Cerdá, A. M. Castro-Luna, C. F. Zinola, C. Kremer, M. E. Martins, J Colloid Interface Sci. 263, 119 (2003).

[85] Zerbino J. O, Castro-Luna A. M., Zinola C. F., Méndez E., Martins M. E, A Comparative Study of Electrochemical and Optical Properties of Rhenium Deposited on Gold and Platinum, J. Braz. Chem. Soc., 2002;13:510-515.

[86] Zerbino J.O, Castro-Luna A.M., Zinola C.F., Méndez E., Martins M.E. Electrochemical and optical study of rhenium layers formed on gold electrodes. J Electroanal Chem 521 (2002) 168–174.

[87] Eduardo C. Muñoz, Ricardo S. Schrebler, Marco A. Orellana, Ricardo Córdova Rhenium electrodeposition process onto p-Si (100) and electrochemical behavior of the hydrogen evolution reaction onto p-Si/Re/0.1 M H2SO4 interface Journal of Electroanalytical Chemistry 611 (2007) 35-42.

[88] Muñoz, E. C., Schrebler, R. S., Grez, P. C., Henríquez, R. G., Heyser, C. A., Verdugo, P. A., & Marotti, R. E. (2009). Rhenium electroless deposition on p-Si (100) from HF solutions under illumination: Hydrogen evolution reaction onto p-Si/Re systems. Journal of Electroanalytical Chemistry, 633(1), 113-120.

[89] Xiaofang Yang, Bruce E. Koel, Hao Wang, Wenhua Chen, Robert A. Bartynski, Nanofaceted C/Re (1121): Fabrication, Structure, and Template for Synthesizing Nanostructured Model Pt Electrocatalyst for Hydrogen Evolution Reaction, ACS Nano 6 (2012) 1404–1409.

[90] Vargas-Uscategui A, Mosquera E, Chornik B, Cifuentes L. Electrocatalysis of the hydrogen evolution reaction by rhenium oxides electrodeposited by pulsed-current. Electrochim Acta 2015; 178:739–47.

[91] Lulu Yang, Shunkai Lu, Hui Wang, Qi Shao, Fan Liao, Mingwang Shao, The self-activation and synergy of amorphous Re nanoparticle – Si nanowire composites for the electrocatalytic hydrogen evolution, Electrochim. Acta 228 (2017) 268.

[92] Gaidelene, J., Kuzmin, A., Purans, J., & Guéry, C. (2005). Influence of hydrogen intercalation on the local structure around Re ions in perovskite-type ReO_3. physica status solidi (c), 2(1), 149-152.

[93] Wang, X., & Andrews, L. (2003). Matrix infrared spectra and density functional theory calculations of manganese and rhenium hydrides. The Journal of Physical Chemistry A, 107(20), 4081-4091.

[94] *It was not possible consulted the original*: K.J. Cathro, Use of platinum-rhenium catalysts for the oxidation of aqueous methanol J. Electrochem. Technol. 5 (1967) 441, *which was cited by*: a) K.J. Cathro, The Oxidation of Water-Soluble Organic

Fuels Using Platinum-Tin Catalysts J. Electrochem. Soc. 116 (1969) 1608; b), K. J. Cathro Fuel Control in Methanol-Air and Formaldehyde-Air Fuel Cell Systems. Journal of The Electrochemical Society, 118 (1971) 1523-1529;c) Attwood, P. A., McNicol, B. D., & Short, R. T. (1980). The electrocatalytic oxidation of methanol in acid electrolyte: preparation and characterization of noble metal electrocatalysts supported on pre-treated carbon-fibre papers. Journal of Applied Electrochemistry, 10(2), 213-222; d) Davenport, William H., Valerie Kollonitsch, and Charles H. Klein, Advances in rhenium catalysts Industrial & Engineering Chemistry 60.11 (1968) 10-19.

[95] Ferrin P, Nilekar AU, Greeley J, Mavrikakis M, Rossmeisl J. Reactivity descriptors for direct methanol fuel cell anode catalysts. Science 602 (2008) 3424–3431, 2008;602:3424–31. Surface.

[96] Garcia-Garcia R, Rivera JG, Antaño-Lopez R, Castañeda-Olivares F, Orozco G. Impedance spectra of the cathodic hydrogen evolution reaction on polycrystalline rhenium. Int J Hydrogen Energy 41 (2016) 4660-9.

Chapter III

Study of Hydrogen evolution reaction, Hydrogen oxidation reaction and Methanol electrooxidation on metallic Rhenium

3.1 Introduction.

To study the electrochemical behavior of rhenium, techniques such as, cyclic voltammetry, linear sweep voltammetry [1] and electrochemical impedance spectroscopy (EIS) [2] were used to focus mainly on the hydrogen evolution reaction on metallic rhenium in acidic aqueous solutions with and without the presence of methanol. The electrodes used were rhenium powder or wire, obtained by metallurgical (fused) methods. The study of rhenium in this work, is divided in two parts: the first one, focused in the HER and HOR on metallic rhenium, meanwhile the second part present a specific study to determine the influence of methanol on the HER and the electrooxidation of methanol on rhenium. The reactions were studied using electrochemical impedance spectroscopy [2] and it is important to mention the lack of experimental data for the electrooxidation of methanol in the literature. These was the principal reason to realize an EIS study at cathodic potentials on the metallic rhenium electrode in acidic solutions without and with methanol.

3.2 Experimental.

3.2.1 Chemical reagents.

Commercial materials and chemical reactants were purchased from several commercials sources and these reagents are listed below:

- Sulphuric acid (H_2SO_4), 98.08%, J.T. Baker.
- Hydrochloric acid (HCl), 99.00%, J.T. Baker
- Rhenium powder, 99.995%, Sigma-Aldrich.
- Rhenium wire, 99.9%, Sigma-Aldrich.
- Platinum wire (99.99 %) Sigma-Aldrich
- Methanol (99.94 %) from J.T. Baker.
- Millipore Milli-Q water (11MΩ cm^{-1}).
- Hydrogen and Nitrogen gas (99.999 %) from Infra Praxair Mexico.
- Nafion® solution 5% wt, from Electrochem.
- Isopropanol (99.99%), Sigma-Aldrich.
- Glassy carbon electrode (GC), BASi®.
- Graphite rod 5mm, Faber-Castell®.

3.2.1 Electrodes.

Platinum wire was used in all experiments as counter electrode, saturated $Hg|Hg_2SO_4|K_2SO_4$ was use as the reference electrode. This electrode was provided by Radiometer analytical (France). Rhenium wire was used as working electrode (geometric area 0.161007cm^2) in most of the experiments. In addition, rhenium as agglomerate was also used as working electrode. The preparation of agglomerate is shown in the diagram on Figure 3.1 and it was made as follows: The rhenium particles (4mg), Nafion® solution (30µL) and isopropanol (30µL) forms a catalyst ink which was sonicated for 30 min. From the close vial with the ink, all the volume was taken and dropped onto the surface of graphitic carbon electrode using a micropipette.

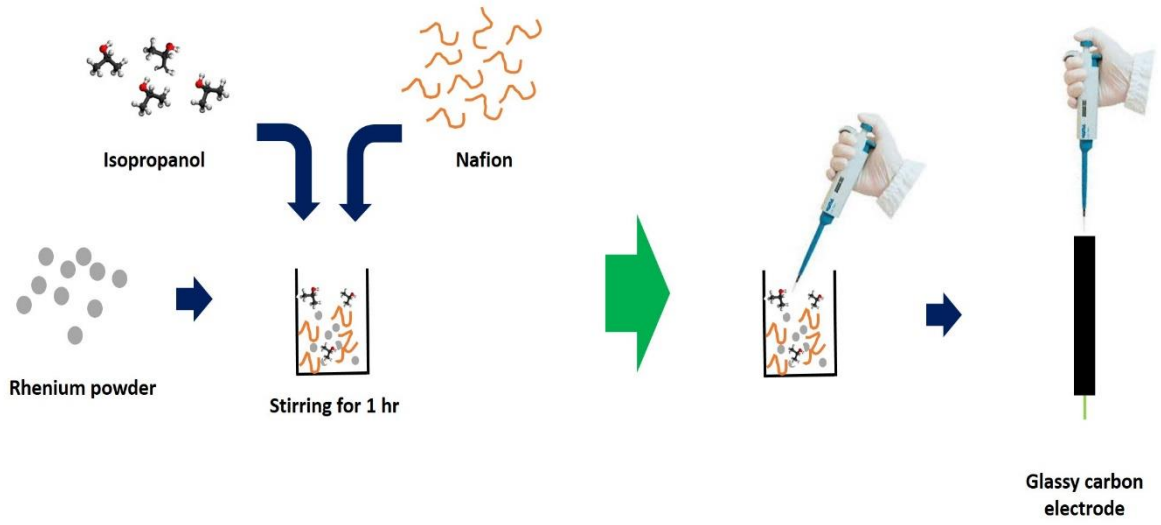

Figure 3.1. Schematic of the preparation of a composite catalytic layer by mixing.

3.2.3 Equipments.

The electrochemical properties of the rhenium electrodes were investigated in the conventional three electrode cell. Three-electrode cell (25mL) was provided by Provitex (Mexico). The schematic experimental setup is shown in Figure 3.2 and the equipment was as follows:

- For impedance measurements, it was used an Autolab model PGSTAT 302 Potentiostat-Galvanostat with a FRA32M module. Seven frequencies per decade were scanned using a sinusoidal potential modulation of 10 mV amplitude peak to peak.

- For the polarization curves and voltammetric technique it was used a BioLogic VSP with EC-Lab® software.

3.3 Experimental conditions.

Before the experiment, rhenium wire electrode was polished on carbide sandpaper (2000 SIC B-99), from Buehler LTD with Al_2O_3 water suspension, particle size 3 - 0.5 μm. The electrolyte was bubbled for 20 min with nitrogen or hydrogen gas before each measurement and during the experiment a gas atmosphere was maintained (Figure 3.1). All the electrochemical experiments were carried out at 22 ± 2 °C and the potentials are reported versus the Normal Hydrogen Electrode (NHE).

3.3.1 Polarization curves.

The electrode was immersed in the dissolution and immediately the applied potential was set at -0.1 V for 1 h, after that, potential sweeps were performed from 0 to 0.1 and from 0 to -0.22 V using scan rates of 0.116, 1 and 10 mV s^{-1}. In another set of experiments after applying a potential of -0.1 V, the potential was suddenly switched to 0.7 V and negative polarization curves were recorded with a scan rate of 1 mV s^{-1}.

3.3.2 Impedance spectroscopy

Alternating current impedance measurements were performed at 0, -0.1, -0.13, -0.2 and -0.3 V. The signal amplitude was 10 mV and the measurements were obtained in the frequency range of 0.1 to 100,000 Hz. The validity of the impedance measurements was demonstrated by performing a Kramers–Kronig transform analysis (pseudo chi-squared values were less than 10^{-5}).

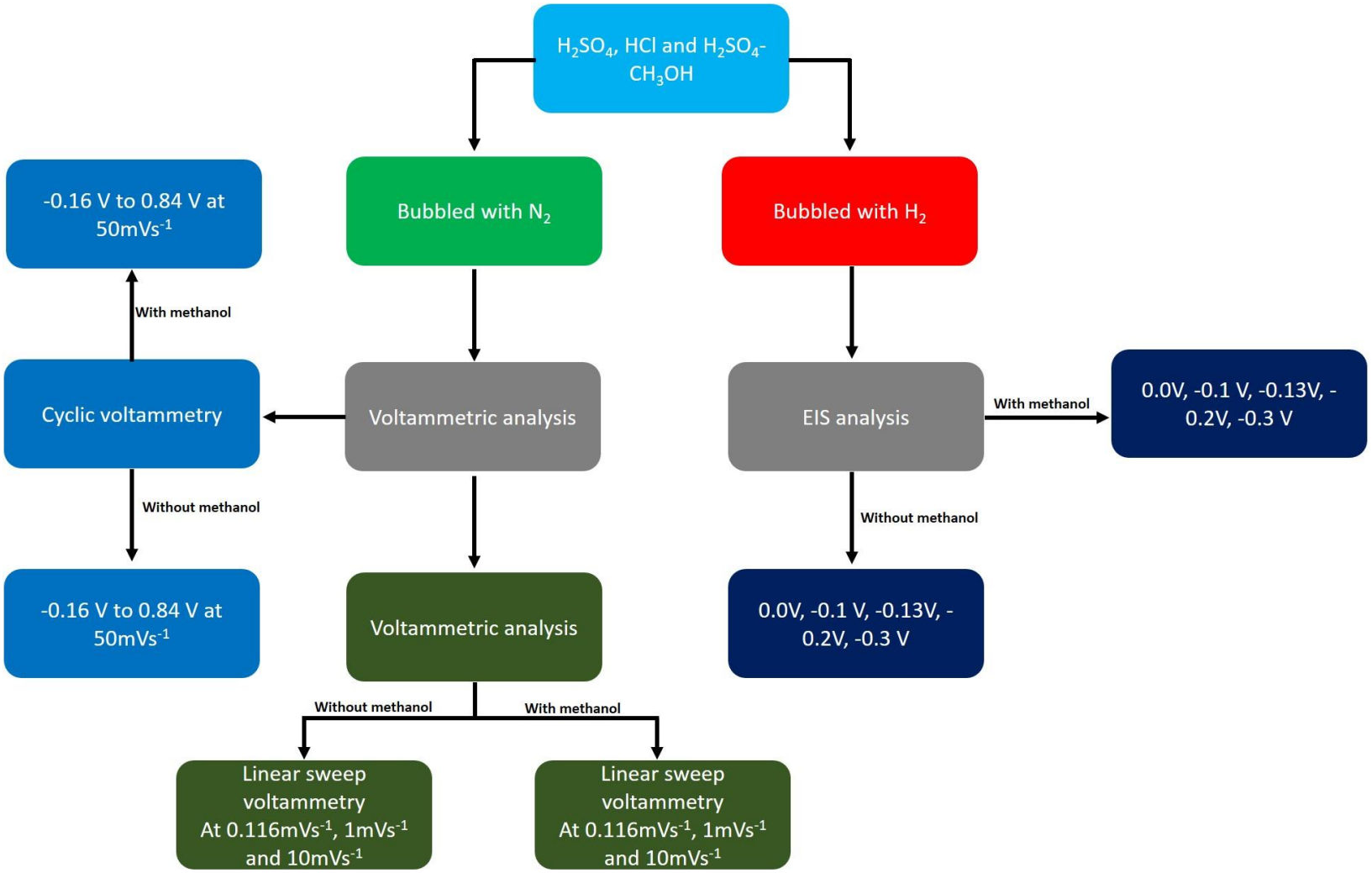

Figure 3.2. A schematic drawing of the experimental set-up.

The equivalent circuit parameters that produce the best fit with respect to the proposed model were performed by running simulations using the Z view 3.0 software. Minimizing errors was done using the chi-squared criteria for fitting the experimental data of the EIS.

3.4 Determination of Exchange Current Density.

The behavior of polarization curves can be described with a Tafel linear comportment [3]:

$$\eta = a + b\log(j) \qquad \text{(Eq. 3.1)}$$

Where, b (Vdec^{-1}) is the Tafel slope, η (V) is the hydrogen evolution overvoltage, j (Acm^2) is the measured current density and a (V) is the intercept related to the exchange current density j_0. The Tafel slope was obtained from the equation 3.2:

$$\mathrm{b} = \frac{-\mathrm{RT}}{\alpha \mathrm{nF}} 2.303 = \frac{0.059\mathrm{V}}{\alpha \mathrm{n}} \qquad \text{(Eq. 3.2)}$$

Where α is the transfer coefficients, R (8.3144621 J K^{-1} mol^{-1}) is the gas constant, F is the Faraday constant (96.485 C mol^{-1}), T is the temperature and n represents the number of electrons exchanged.

The Tafel slope states the actual properties of an electrocatalyst and it was obtained from the linear part of the polarization curves. By plotting log j vs. η, a linear extrapolation to an intercept in Y axis, is easy obtain the of log j_0 value.

3.5 Estimation of Exchange Current Density.

In section 2.3, with Eq. 2.28 the exchange current density of HER on metallic rhenium and others metals can be calculate, using metal work function values. When, the fundamental constants are substituted appropriately and the temperature was at 298 K, it can be obtained:

$$j_0 = 9.9\mathrm{x}10^{-7}\left(\frac{\mathrm{C_{H+}}}{\mathrm{A}}\right)\exp\left\{-38.9 + 6.6\Phi_{\mathrm{M}}\right\} \qquad \text{(Eq. 3.3)}$$

Where:

j_0 = exchange current density for HER on the metal

$C_{H+} = 1M$ or $C_{H+} = 0.5M$, Molar concentration of H^+ ions, represented in moles

A = 0.001 cm^{-2} the electrode area

Φ_M = is the work function of the metal.

3.6 Results.

3.6.1 Rhenium Electroactivity towards the HER and HOR.

Figure 3.3 shows that the anodic current of HOR is negligible and a very small pair of peaks are observed around 0.2 V. This pair peaks are placed in the predominance zone of ReO_2 and according to the predominance diagram these peaks can be attributed to ReO_2. The pair peaks were assigned to the under-potentially deposited hydrogen, (UDP-H) by Chun et alt. [4], while, Gómez [5] assigned them to the Re/ReO_2 redox couple. In accordance with the predominance diagram (Figure 2.1) these peaks can be assigned to Re/ReO_2 couple. The surface analysis will be explored in future research to verify this postulate. The experimental voltammogram is similar than the results reported in others works [6,7].

Transition elements in the periodic table such Pt, Ir and Os shows peaks for HOR between 0 to 0.25 V [8,9], that does not appear on the rhenium voltammogram (Figure 3.3). In addition, it is difficult to identify the UDP-H on Figure 3.3. In section 1.2 it was commented, that several studies suppose that HOR and HER are reversible reactions on rhenium [9]. Consequently, the j_0 was supposed to be equal for HER and HOR, however the experimental results do not support this assumption.

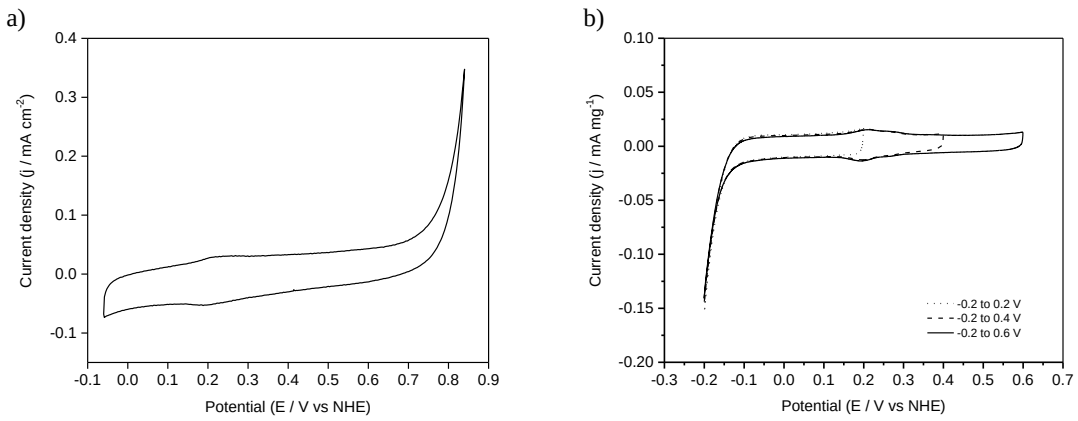

Figure 3.3. a) Re wire voltammogram and b) Rhenium powder electrode, cycle 15, in H_2SO_4 0.5 M bubbled whit N_2, at 50 mVs^{-1}.

Garcia [6] commented the possible influence of oxide in the HER response, this can produce a high value of j_0. In this regard, the experimental results in Figure 3.4. were conducted for comparison. The hydrogen gas was bubbled in the solutions and -0.1 V vs NHE was applied during a 2hr, the H_2 bubble formation at the surface electrode was not observed. Suddenly the potential was switched to -0.2 V or 0.8 V. The current value at the start potential was very high. This high value can be attributed principally to the double layer charging, however in both curves some percentage of the current can be assigned to the formation of a soluble rhenium oxide (Eq. 2.7). It is hard to accept that HOR occurs with huge overpotential and their current is convoluted with the current produced by the oxidation of rhenium. On the other hand, the HER current appears in both curves (Figure 3.4) approximately at 0.0 V and there is a slight increase of the current in presence of soluble oxide, which can be related to the increase of surface roughness, when the new surface is formed by the dissolution of the electrode. In the anodic curve, a very small peak (inset plot Figure 3.4) is observed at -0.05 V and this feature might be related to bubble detachment, which was formed in the cathodic pre-polarization. It is difficult to consider the HOR as the cause of this feature. Gómez [5] observed some peaks on an anodic curve at high acid concentrations (pH -0.7 V) which was assigned to the HOR.

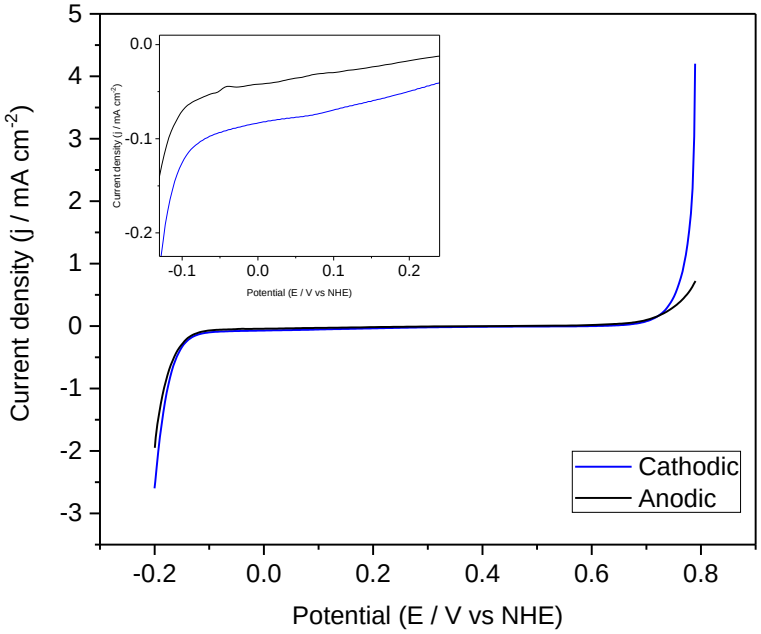

Figure 3.4. Polarization curves of metallic rhenium (wire) in 0.5 M H_2SO_4, scan rate:1mVs^{-1}, inset plot shows a zoom between -0,1 to 0.2 V. Before the polarization curve the potential was hold at -0.21 V during 2 hr and a fresh electrode was used in each sweep.

To support a supposition of small interactions between metallic Re and hydrogen gas, it was observed that rhenium at high temperature do not react with this gas [10,11]. Grgur [12], suggest that rhenium has poorly sites for the hydrogen electrooxidation,. So, this work found a high inactivity of rhenium towards the HOR. . It is necesary comment the fact that the H_2 chemisorption on PtRe is inferior than the chemisorption upon Pt King [13], so Re alone can shows lower Hads then Pt or PtRe, this is observed in the Figure 3.4. Polarization curves were made at low scan rate to find the value of the j_0 for Hydrogen Evolution Reaction on rhenium electrode. Figure 3.5 shows an example of the E–log (j) plots of rhenium in acid dissolutions. It can be inferred that the HER starts around −0.11 V vs NHE. On polarization curves bubbles of gas were observed at -0.55 V, mainly when the scan rate was at 0.166 mV/s.

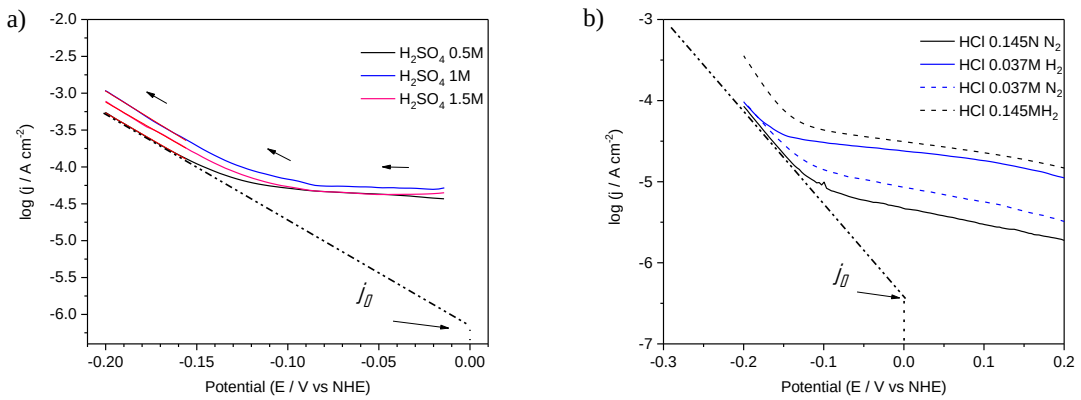

Figure 3.5. a) Potential-Log i plot for Re wire in different concentrations of HCl bubbled with H_2. Scan rate, 1 mVs^{-1}. b) Polarization curves in HCl solutions bubbled with N_2 and H_2. Scan rate, 0.116 mVs^{-1}.

The linear polarization was carried out in two different acids HCl, and H_2SO_4. The results are display in Figure 3.5, after the measurements the linear range was fitted and the results are shown in Table 3.1 which contains the average of interchange current densities obtained from the experimental potential–log current plots. The experimental values of the exchange current densities, are in agreement with previous studies [6].

Figure 3.6, shows a E–log (j) plots, recorded at different polarization direction. There are slight differences in the HER region in both plots and their exchange currents in the linear region were analogous. Moreover, the same tafel slope was observed independently the direction. In addition, the exchange current density values are similar to the values enlisted in Table 3.1. This implies that the soluble oxide slightly influences the HER. Now it recalls the comment of Gómez et al [5], who mentioned that the HER current can be convoluted with the current of the electrodeposition of the anion rhenide (Eq. 1.3).

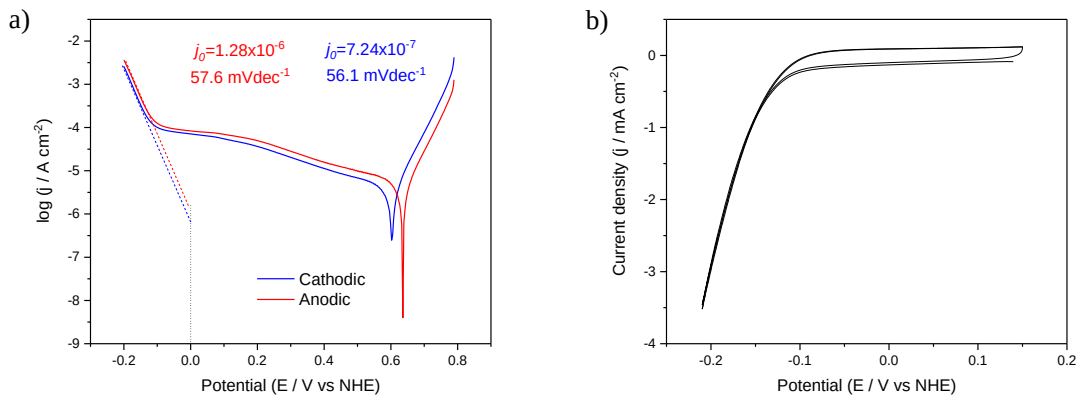

Figure 3.6. Potential–log (j) plots at scan rate at 1 mVs^{-1}and cyclic voltammogram at 10 mVs^{-1} in 0.5 M H_2SO_4.

This suggestion was made based on the influence of the stirring rate in the solution over the currents, when the voltammograms have an upper limit at 0.6 or 0.8 V. Then, the soluble species may explain the dependence with the stirring rate of solution observed for Gómez [5]. Although Figure 3.6 displays that the switching potential produce a hysteresis in the potential–log current plots, the electrodeposition of soluble oxide cannot affect the HER. This hysteresis could be caused by the change of surface roughness as commented above. This seems to suggest that the oxide molecules were not reduced to metallic rhenium on the surface electrode, which is the metallurgical rhenium. In the mechanism of electrodeposition, a complete reduction of ReO_4 to metallic rhenium was not observed [14,15]. In any case, the possible adsorption of these oxides covers a very small surface area that did not affect the HER.

The j_0 value in HCl dissolutions is similar to the value in H_2SO_4 dissolutions at different concentrations (Table 3.1). Considering the difference in electrolytes composition among different experimentations, the average of exchange current density is: j_0=1.6×10^{-6} ± 2.43×10^{-6} Acm^{-2}, this value obtained in this research is very close to the value reported in literature (7.3×10^{-6} Acm^{-2} [8], 2.1×10^{-5} Acm^{-2} [9] and 8×10^{-6} Acm^{-2} [7]). In addition, a variation of the Tafel slopes values was observed from 52 mV dec^{-1} to 60 mV dec^{-1}.

Table 3.1. Current density values averages obtained at different scan rate, solutions, gas bubbled and windows potential range.

Solution	Scan rate mVs^{-1}	j_0 / Acm^{-2}	Reference
0.037 M HCl, H_2	1	$4.4\times10^{-7}\pm1.48\times10^{-7}$	[6]
0.037 M HCl, H_2	0.116	$1.22\times10^{-6}\pm1.10\times10^{-6}$	[6]
0.145 M HCl, H_2	1	$3.29\times10^{-7}\pm7.41\times10^{-7}$	[6]
0.145 M HCl, H_2	0.116	$2.02\times10^{-6}\pm9.13\times10^{-7}$	[6]
0.5 M H_2SO_4, H_2	10	$1.21\times10^{-6}\pm9.58\times10^{-7}$	[6]
0.5 M H_2SO_4, H_2	1	$6.51\times10^{-7}\pm4.28\times10^{-7}$	[6]
0.5 M H_2SO_4, H_2	0.116	$8.10\times10^{-7}\pm3.55\times10^{-7}$	[6]
1.0 M H_2SO_4, H_2	1	$7.85\times10^{-7}\pm5.54\times10^{-7}$	[7]
1.0 M H_2SO_4, H_2	0.116	$5.91\times10^{-7}\pm4.90\times10^{-7}$	[7]
1.5 M H_2SO_4, H_2	1	$7.22\times10^{-6}\pm2.09\times10^{-6}$	[7]
1.5 M H_2SO_4, H_2	0.116	$7.94\times10^{-6}\pm2.14\times10^{-6}$	[7]
0.5 M H_2SO_4, N_2	1	$4.31\times10^{-7}\pm4.12\times10^{-7}$	This work
0.5 M H_2SO_4, N_2	0.116	$8.29\times10^{-7}\pm2.49\times10^{-7}$	This work
1.0 M H_2SO_4, N_2	1	$8.34\times10^{-7}\pm3.48\times10^{-7}$	This work
1.0 M H_2SO_4, N_2	0.116	$4.30\times10^{-7}\pm2.86\times10^{-7}$	This work
1.5 M H_2SO_4, N_2	1	$2.61\times10^{-7}\pm1.10\times10^{-7}$	This work
1.5 M H_2SO_4, N_2	0.116	$2.87\times10^{-7}\pm1.95\times10^{-7}$	This work
0.037 M HCl, N_2	1	$5.33\times10^{-7}\pm5.33\times10^{-7}$	This work
0.037 M HCl, N_2	0.116	$5.79\times10^{-7}\pm1.88\times10^{-7}$	This work
0.145 M HCl, N_2	10	$7.11\times10^{-7}\pm6.13\times10^{-7}$	This work
0.145 M HCl, N_2	1	$3.46\times10^{-7}\pm2.32\times10^{-8}$	This work
0.145 M HCl, N_2	0.116	$5.36\times10^{-7}\pm1.95\times10^{-7}$	This work

In the section 2.3 a comparison between exchange current of rhenized surfaces and metallurgical rhenium was pointed. In this regard, Krasikov [16] remarked that the electrochemical reduction of rhenium from soluble oxides is complicate. (for example, H_xReO_3 [17] or $H(ReO_4)$ H_2O [18–20]), and this bronzes could increase the performance of the HER on rhenium. However, the j_0 reported for electrodeposited rhenium in alkaline media is 2.4 $\times 10^{-6}$ Acm^{-2} [15], which is very close to the exchange current determined in this work.

Currently, the data considering that rhenium possesses the same electrocatalytic activity than platinum cause confusion in theoretical studies. In section 2.3 the study of Andreev [21] was commented, the values he calculed for Re and Pt have similar performance for the HER, despite the fact these elements have a different surface energy, this results as a contradiction. The experimental results obtained (Table 3.1) can delete this incongruity commented about the work of Andreev [21]. In addition, the experimental value of j_0 (1.6×10^{-6} Acm^{-2}) resolves discrepancies presented in Figures 2.4 and 2.5. The experimental results obtained suggest that rhenium follows the Sabatier Principle, which established that low and very high energies of hydrogen adsorption on metals produce lower performances meanwhile intermedia energy produces a high performance of platinum for the HER.

In section 2.3, the linear behavior between log j_0 and the work functions. The study was focused on the 6th period elements of the periodic table (Pt, Ir, Os, Re, W and Ta). The Φ-coordinate and log j_0-coordinate selected values for each 6-th period element, except for Re. It follows that the log j_0-coordinate of Re, can be calculated using Eq. 3.2. Naturally, in the selection of log j_0-coordinate it is considered the average of experimental results 1.6×10^{-6} Acm^{-2}. Consequently, it was selected that the Φ-coordinates are 4.87 eV and -5.93, see Table 2.4 in Chapter 2. Then, the results were plotted, so the Φ-coordinate and log j_0-coordinate for each element of the 6th period in Figure 3.7 could be compared. To compare the different values of exchange current density reported in the literature, the log j_0 reported by Appleby and Kita [22], Pecherskaya [23] and Krasikov [24] are also included. A linear fit

was performed and the r^2 value of each linear regression provides a measurement of how well the trend-line approximates the real data points. Consequently, the value of r^2 0.9711 obtained with our value of log j_0 is closer to the trend-line than the value of 0.73605 obtained using the value reported by Pecherskaya [23]. Also, the linear regression with data from Krasikov [24] displays a linear trend (r^2 0.9547). This result strongly suggest that rhenium follow the Sabatier Principle.

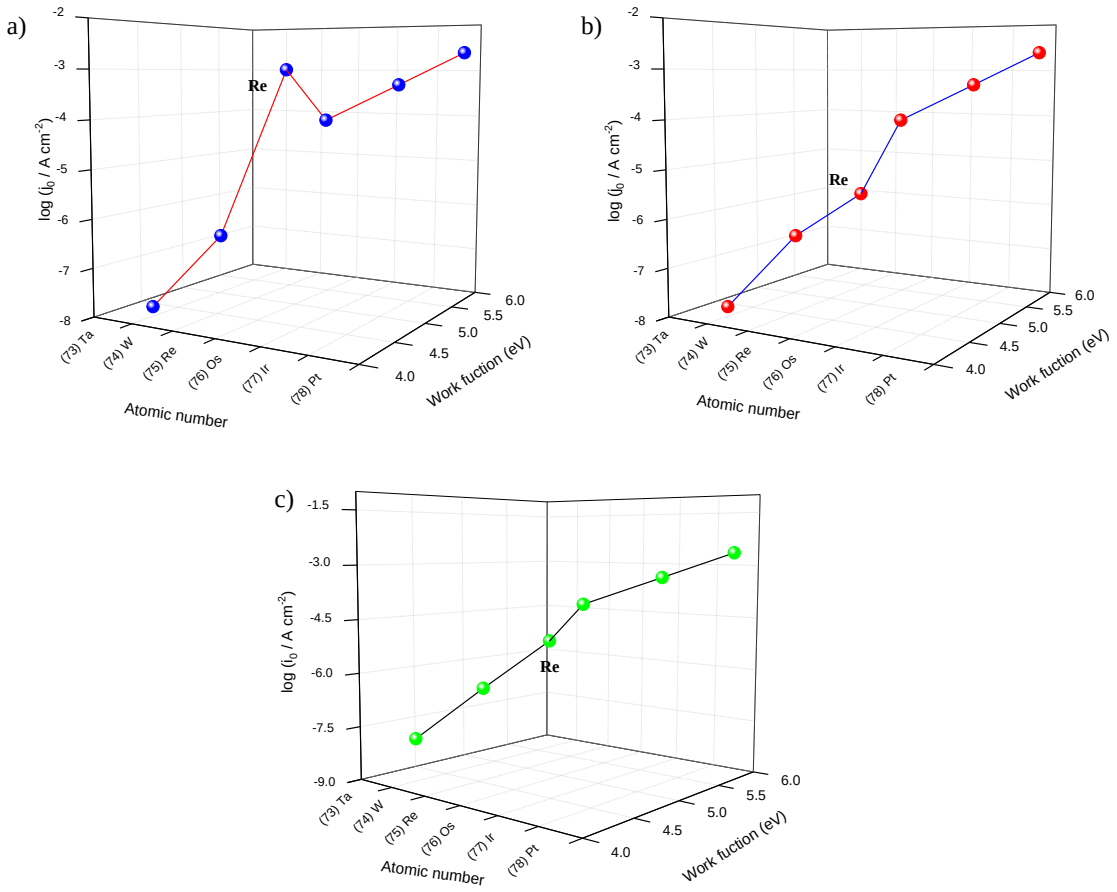

Figure 3.7. Exchange currents for Hydrogen Evolution Reaction (j_0) vs. values of the work function of elements of the sixth period of the periodic table. a) —●— Pecherskaya, b) —●— log j_0 value this work, c) —●—. Krasikov value.

It is important to mention that the determination of tafel slope of HER is difficult in Figures 3.5 and 3.6**,** that is, there is uncertainty in the onset and end-points locations due that the common tafel plot with cathodic and anodic branch is no

easy to identify in the results founded , so the tafel slope was determinate with the thermodynamic potential 0.0V for HER. For example, Joncich [25] choice the end-point at 0.0 V and the start-point approximately at -0.15 V, that is, this author worn in an effort to stop the line from progressing to greater degrees of curvature. This study assumed the value of 0.0 V as ended potential and start-potentials from the linear region. Then, in Table 3.1 the current tabulated corresponds to the potential at 0.0 V, which is the thermodynamic potential of the HER. This assumption permits to estimate a reliable data of the kinetics of the HER on rhenium.

The activity observed for Rhenium in this work compared with Muñoz [26] results for , p-Si/Re electrode is lower. Schrebler [27] determined on p-Si /Re contained rhenium oxide, and this activity is for rhenium oxides. However the determinate activity for HER on metallic rhenium suggest that this electrode does not contain oxides.

It was commented in section 2.3 that Trasatti [28] determined the linear correlation in Eq. 2.29 using data for several metals, including rhenium. In Figure 3.8 the predicted log j_0 with equation 2.29 displays a linear comportment (dash and blue line) with similar pattern that the behavior observed from the experimental log j_0 and selected work function in section 2.3 (dotted red line with black square). It is important to note that the quantitative relation between log j_0 and the work function depend on the values reported, in this case different values were used. Then, the line calculated with Eq. 2.29 overestimated the currents with the work functions selected in section 2.3. Nevertheless, a linear behavior can be established for the *d* metals in the 6th period with the experimental data obtained in this work. To clarify, in this correlation Au was not considered. The three coinage metals (Au, Ag, Cu) show an ordinary electrocatalysts performance for HER because the position of their *d* bands is unfavorable for the hydrogen adsorption.

The experimental j_0 value (red star) fit accurately in the lineal behavior and conversely j_0 reported by Pecherskaya [23] (∆) do not follows the tendency. Figure 3.8, also includes the log j_0 reported by Krasikov [16] for HER (symbol empty square) and this value also fit in the trend-line. Figure 3.8 reaffirm that the log j_0-

coordinate and Φ-coordinates are 4.87 eV, -5.939, respectively. These values can be used as an appropriate value of HER on metallic Rhenium.

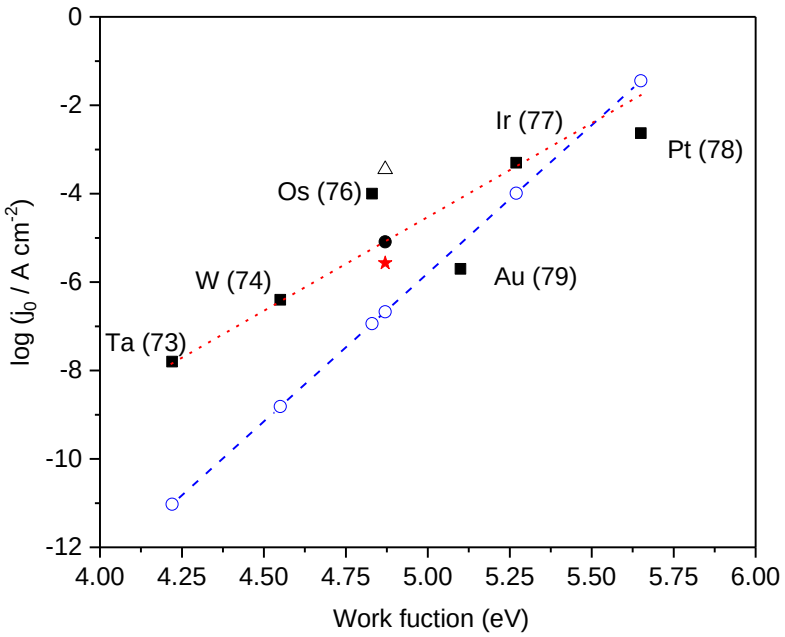

Figure 3.8. Log j_0 versus work function reported in Table 2.4. Dashed and blue line with empty circles is the Trasatti Eq.2.29 [28]. Red and dotted line with symbol square is the Φ-coordinate and logj_0-coordinate selected values. j_0 values for rhenium: (△) Pecherskaya [23],. (●) Krasikov [16] and (★) this work result.

3.6.2 Rhenium Electroactivity towards the methanol electro-oxidation and their influence in the HER

The DFT study of Ferrin [29] predicts that rhenium and ruthenium facilitate the methanol electrooxidation to CO by the bifunctional mechanism, rhenium oxides easy permit the water dissociation and the adsorption of OH species as Ru does. Consequently, methanol electrooxidation was expected to be detected in the rhenium cyclic voltammetry analysis. Conversely, it was found that methanol is not electrooxidized on rhenium surface, this means that Ferrin [29] prediction it is not completely right due to the experimental results obtained, see Figure 3.9. Usually the methanol electrooxidation begins at 5.0 V vs NHE [30] on platinum-ruthenium alloys, in contrast the voltammogram (Figure 3.9) does not display differences with

or without methanol in the dissolution. It was not possible read the original work of Cathro [31], but Davenport [32] reported that metallic rhenium did not support anodic current.

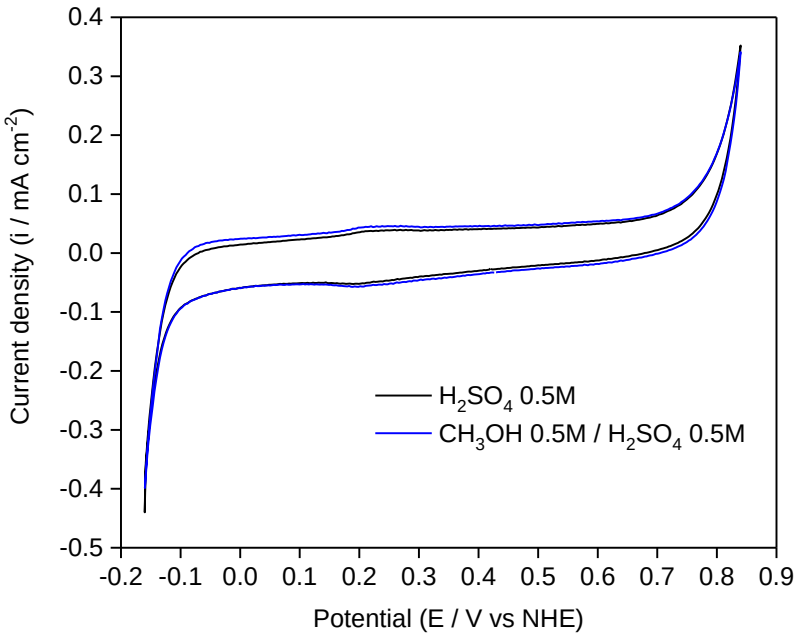

Figure 3.9. Re wire voltammogram, cycle 15 in methanol presence at 50mVs^{-1}, dissolutions bubbled with N_2 before the experiment.

To determinate the methanol influence on the HER, when this is added to the dissolution, different concentrations were carried out, the polarization curves were recorded at different scan rates and Figures 3.10-3.12 displays the experimental results obtained. The cathodic currents stars at -0.1 V, which is an inflexion point in the curve and a linear behavior appeared. The j_0 obtained from electrodes immersed in solutions with methanol are in the same order of magnitude than in acid media without this alcohol, see Table 3.1 (without methanol) and Table 3.2 (with methanol). It was commented above that the tafel slope in acid solutions was approximately 60 mV dec^{-1} very similar to the values observed in acid media with methanol. These slopes are found to increase slightly with methanol concentration from 60 mVdec^{-1} to 67 mVdec^{-1}, but they can be assigned to the same mechanics. To establish the influence of methanol on the HER, each value of methanol

concentrations was converted to percentage (%V/V) and plotted against j_0 average in Figure 3.13. The effect of methanol in j_0 is similar to the observed by Bockris [33] for severals metals, were the j_0 decreases when the methanol concentration increases. Since the differences between exchange current measurements in solutions with or without methanol are very small, it can be inferred that methanol imposes little influence on the HER on rhenium. Although, the exchange current decreased half an order of magnitude lower in than exchange current obtained for HER on rhenium in dissolutions without methanol, is quite different from the behavior observed for platinum-group metals [34].

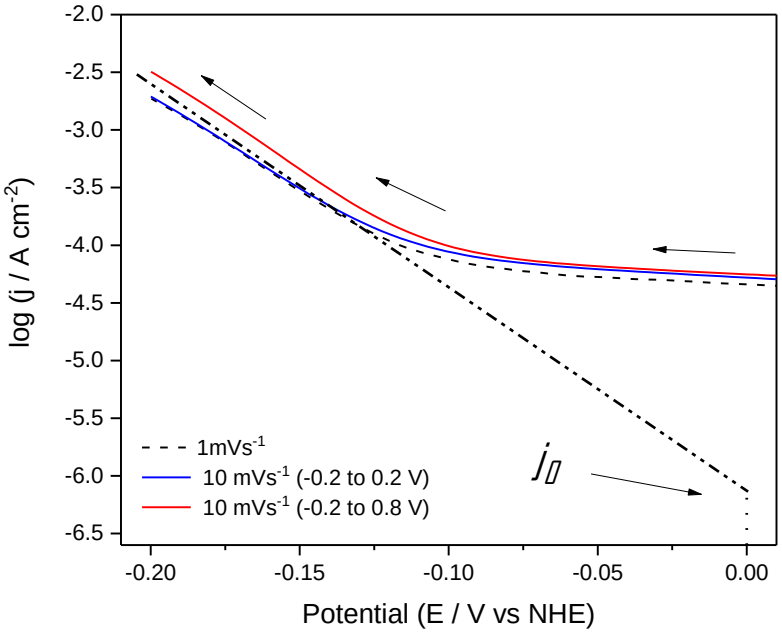

Figure 3.10. Potential-Log j plot for Re in CH_3OH 2 M /H_2SO_4 0.5 M bubbled with H_2, at different scan rates.

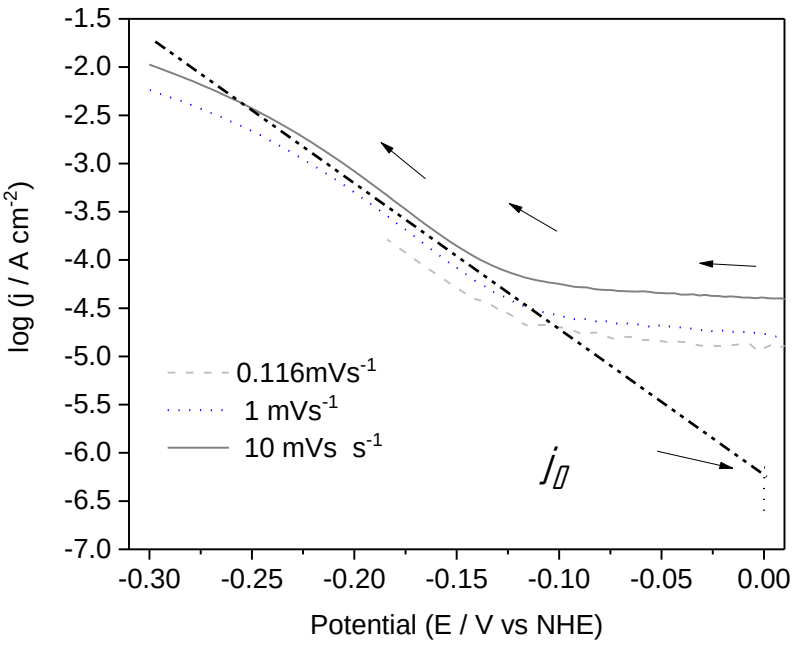

Figure 3.11. Potential-Log j plot for Re in CH_3OH 1 M /H_2SO_4 0.5 M bubbled with H_2, at different scan rates.

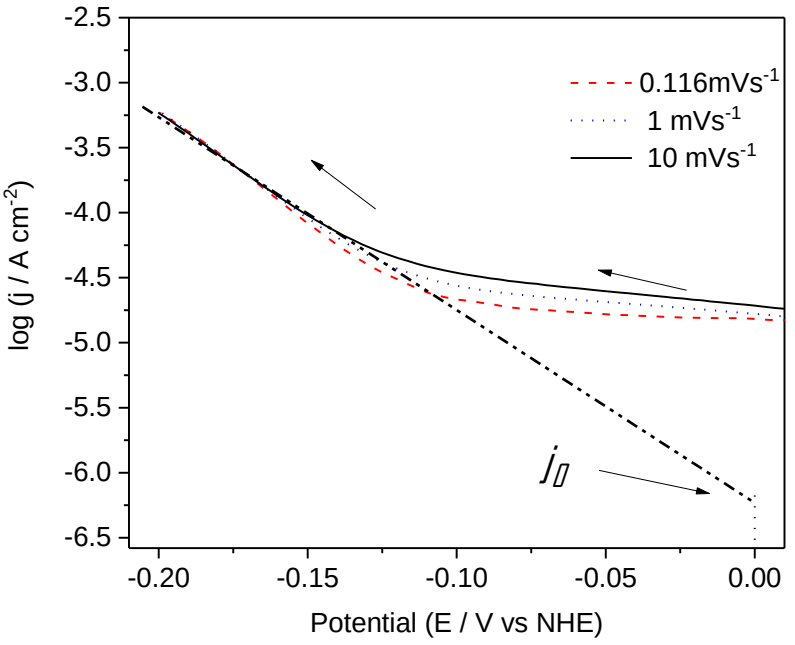

Figure 3.12. Potential-Log i plot for Re in CH_3OH 0.5 M / H_2SO_4 0.5 M bubbled with H_2, at different scan rates.

Table 3.2. Kinetics parameters for HER determined at different methanol concentrations. The j_0 and tafel slopes values were determined from the dotted line in each Figure using the equation 3.1 and 3.2.

Solution	Scan rate mVs^{-1}	Log j_0 ($A\ cm^{-2}$)	Tafel slope ($mVdec^{-1}$)
0.5 M CH_3OH, H_2	0.116	-6.67	57.8
0.5 M CH_3OH, H_2	1	-6.52	60.06
0.5 M CH_3OH, H_2	10	-6.38	63.5
0.5 M CH_3OH, N_2	0.116	-6.54	56.2
0.5 M CH_3OH, N_2	1	-6.33	56.3
0.5 M CH_3OH, N_2	10	-6.18	59.4
1 M CH_3OH, N_2	0.116	-6.43	68.6
1 M CH_3OH, N_2	1	-6.06	67.4
1 M CH_3OH, N_2	10	-6.03	68.2
2 M CH_3OH, H_2	1	-5.94	61.9
2 M CH_3OH, H_2	10	-5.87	63.1
2 M CH_3OH, H_2	10	-5.85	59
2 M CH_3OH, N_2	0.116	-6.36	61.9
2 M CH_3OH, N_2	10	-6.08	61.5
2 M CH_3OH, N_2	10	-6.21	55.2
2 M CH_3OH, N_2	10	-6.21	55.2

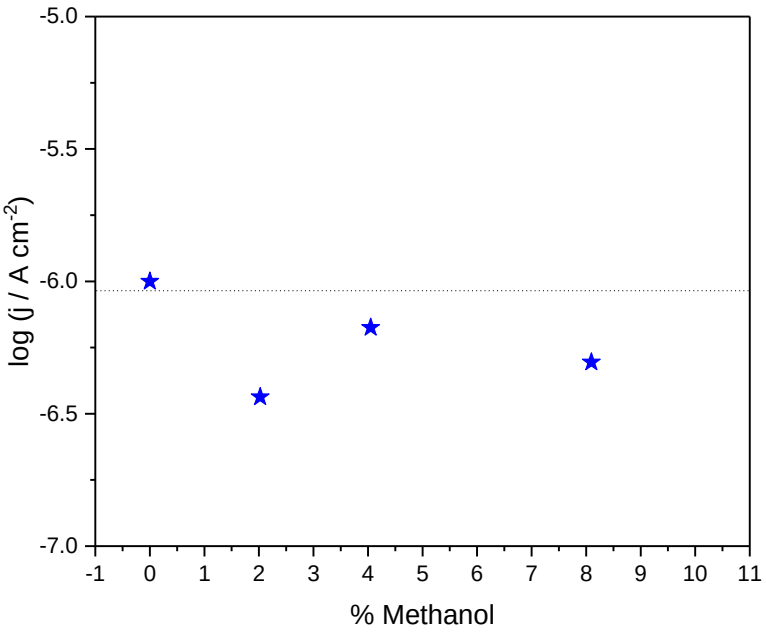

Figure 3.13. Change of log j_0 at different methanol percentage.

3.7 EIS study of Hydrogen Evolution Reaction on Rhenium in presence of methanol

The Nyquist spectra in acid solutions without methanol were recorded for comparison. The impedance plots exhibit a semicircle in the explored frequency range (Figure 3.14a). Then, the equivalent circuit (Randles) can be proposed to explain the behavior of rhenium electrode at cathodic potential. The circuit includes a solution resistance, (Rs), a constant phase element (CPE, defined by CPE-T and CPE-P) in parallel with a polarization resistance or charge-transfer resistance (R_{CT}), then fitted parameters for the equivalent circuits are enlisted in Table 3.3. Bode plots (Figure 3.14c) and phase plots display that the solution resistances were influenced by HCl concentration. As can be expected, when the number of ions in the solution increased the resistance decreased. This spectra comportment is quite similar to that reported by Garcia [7] and Chun [4,35,36].

The Nyquist plots obtained in dissolutions with methanol at several cathodic potentials display a complete semicircle. There is greater R_{CT} in presence of

methanol (Table 3.4) compared with solutions without this alcohol (Table 3.4), which can be explained for the formation of hydrogen bonds between methanol and water, which decreases the number of protons.

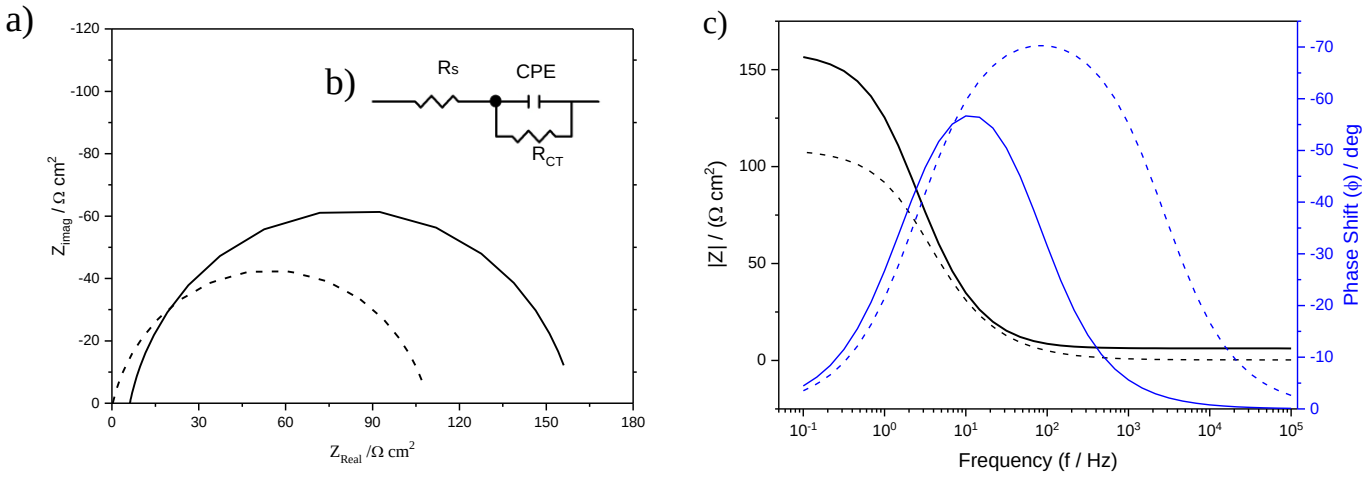

Figure 3.14. a) Nyquist plot, c) bode plot of wire electrode of metallic rhenium continue line in HCl 0.037 M and dashed line in HCl 0.145M. The spectra were obtained at -0.15 V vs NHE. Nitrogen was bubbling with stirring for 15 min beforehand. Each potential was applied (pre-polarization) for 15 min before the impedance spectra collection at -0.15 V, b) equivalent circuit (Randles) proposed for the rhenium electrode.

The different values of R_{CT} tend to decrease at more negative potentials and this can be observed in the Table 3.4. It can be postulated that some ions are formed after the discharge of proton into surface according to the reactions in Eq. 3.4 to 3.8. In Eq. 3.4 it is easy discarded because the speciation diagram of sulfuric acid normally reported [37] displays that the predominance species (97%) is hydrogen-sulfate (also known as bisulfate for historical reasons). The increased of sulfate ions (Eq. 3.5) can be explained by the increment in the conductance of the solutions. The reactions from Eq. 3.6 to 3.8 can occur at very concentrated acid [38,39] and then they are improbable in our experimental conditions.

$$H_2SO_4 + H_2O \leftrightarrow HSO_4^- + H_3O^+ \qquad \text{(Eq. 3.4)}$$

$$HSO_4^- + H_2O \leftrightarrow SO_4^{2-} + H_3O^+ \qquad \text{(Eq. 3.5)}$$

$$ROH + H_3O^+ \leftrightarrow ROH_2^+ + H_2O \qquad \text{(Eq. 3.6)}$$

$$H_2SO_4^- + ROH + H_3O^+ \leftrightarrow ROSO_3H + 2H_2O \quad \text{(Eq. 3.7)}$$

$$ROSO_3H + H_2O \leftrightarrow ROSO_3^- + H_3O^+ \quad \text{(Eq. 3.8)}$$

Table 3.3. Impedance parameters values obtained by fitting Randles (Rs(R_{CT}CPE)) circuit equivalent electrical circuits with ZView software®. The electrode was a rhenium wire.

Solution M HCl	Gas bubble	E (V)	χ2	Rs ohms cm2	Rct Ohms cm^2	CPE μF/cm^2
0.037	N_2	-0.15	7.411×10^{-9}	1.24	160.48	6.2109E-6
0.037	H_2	-0.15	2.118×10^{-9}	1.43	292.73	6.211E-6
0.145	N_2	-0.15	1.623×10^{-9}	0.36	103.09	6.2108E-6
0.145	H_2	-0.15	6.359×10^{-9}	0.35	178.52	6.211E-6

More experiments were carried out and the results are presented in Appendix A. In accordance with the values in Table 3.4 and Appendix A, the circuit of Randles adjusts successfully to the diagrams obtained from EIS measurements. The spectra at several potentials are very similar and comparable, the R_{CT} (3-10 Ωcm^2) is obtained in these potentials. The presence of methanol affects directly the charge-transfer resistance (R_{CT}), however it is hard to explain this decrement in the presence of methanol. If adsorption occurs in the surface like other metals [34] then the electrooxidation can occur at high over-potentials. In addition, the Tafel slope and consequently the mechanism could be affected. But, that was not the case. An alternative is the formation of sulfuric-acid− methanol−water complexes [40] It is well-know that methanol causes severe structural changes in liquid water due to the strong interactions of water with methanol [41].

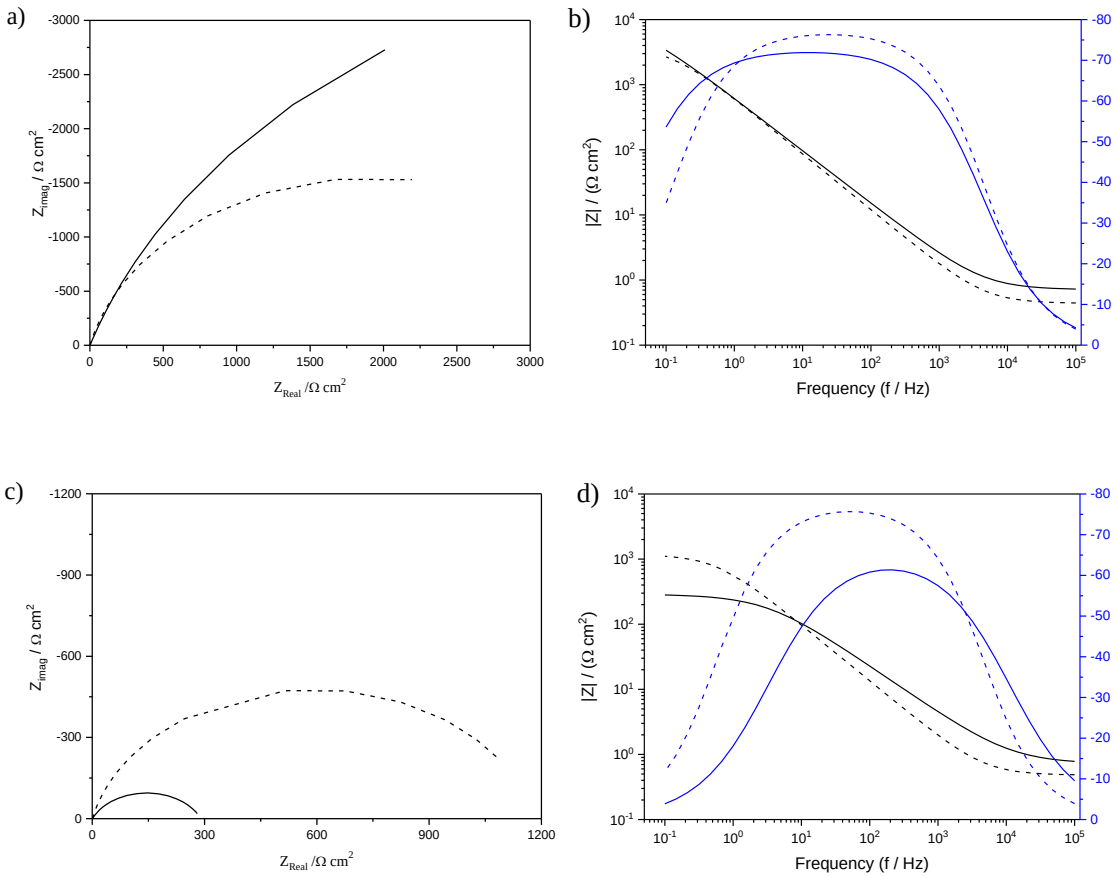

Figure 3.15. Nyquist plot and bode plot of wire electrode of metallic rhenium. The spectra were obtained at 0.0 V (a, b) and -0.1V (c, d),. Hydrogen was bubbling with stirring for 15 min beforehand in the H_2SO_4 0.5 M (solid line) and CH_3OH 1 M /H_2SO_4 0.5 M (dashed line) solutions.

Consequently, the sphere of solvation of hydrogen-sulfate could be in the immediate neighborhood of the primary solvation of hydroxyl groups of methanol. This structure of sulfuric-acid−methanol−water solvation shells, does not affect the water-water hydrogen bonds and their adsorption process, but decreases the number of protons in the interface.

The results found in this section indicate the following issues:

a) The calculations made by Ferrin [29] with regards to mechanism for the methanol electrooxidation on metallic rhenium are not confirmed by the results above; that is opposed to the predictions of a stepwise dehydrogenation of CH_3OH on rhenium between 0.4-0.8 V, the voltammograms do not show features that can be assigned to this process. In this regard, Nikonova [42] and Chang [43]

commented that only oxides with high oxidation states (V-VII) can react with methanol and not the oxides with oxidation states (II-IV), which are the oxides that predominate at these potentials, see Pourbaix diagram in Fig. 2.1a.

b) Any evidence has been found about the electrooxidation of methanol to CO_2 proceeds through the $CO_{(ads)}$.

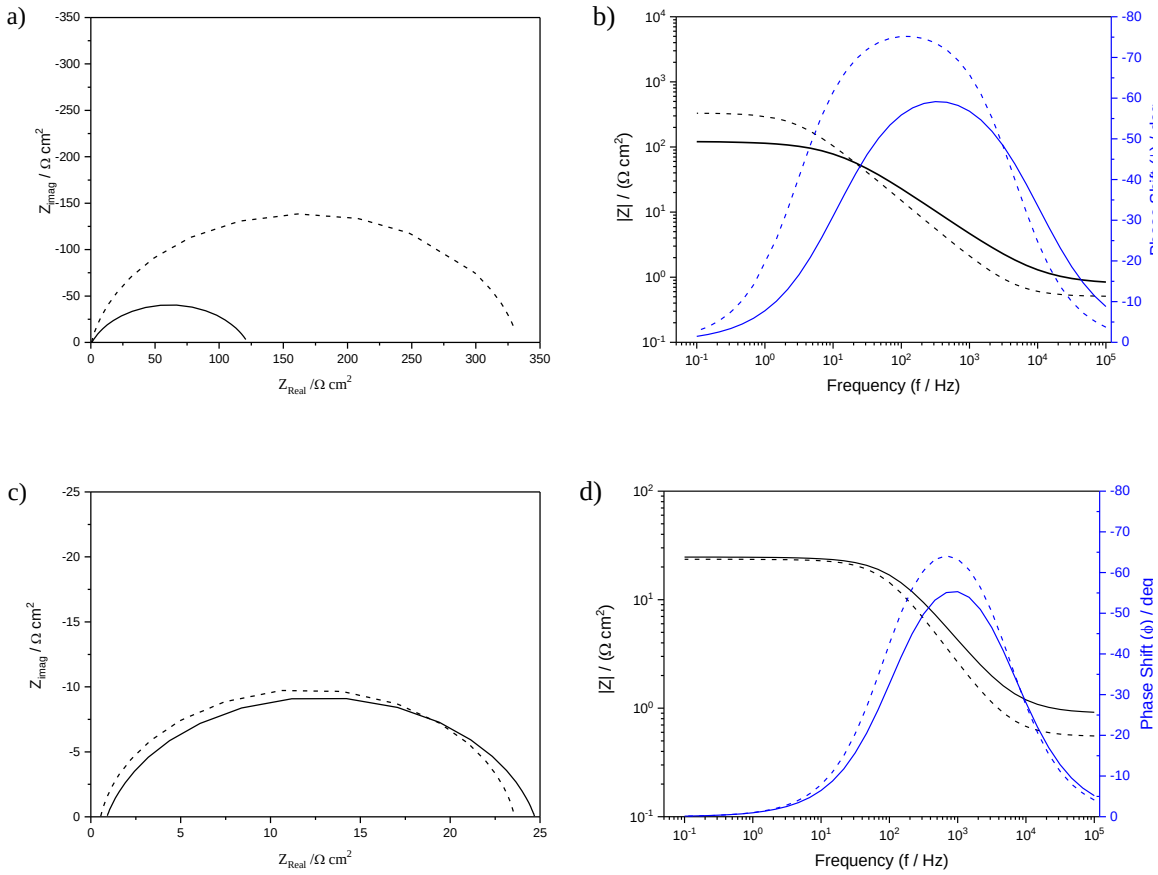

Figure 3.16. Nyquist plot and bode plot of wire electrode of metallic rhenium. The spectra were obtained at -0.13 V (a, b) and -0.2 V (c, d). Hydrogen was bubbling with stirring for 15 min beforehand in the H_2SO_4 0.5 M (solid line) and CH_3OH 1 M /H_2SO_4 0.5 M (dashed line) solutions.

c) The theoretical studies of Anderson [44] and Ferrin [29] show that Os, Pd, Ru, Co, and Re bind H_2O with stronger energy than Pt, and conversely Rh, Ni and Ir bind with less energy. In this group, rhenium is the only metal with negative value of free energy of adsorption. Therefore, the strength of the $Re\text{-}OH_{(ads)}$ bond was sufficiently stable and there is not interaction between methanol and rhenium

surface. Ferrin [29] suggested that the oxygen poisoning could be a problem for rhenium metal with very strong OH binding. In fact, that oxygen poisoning prevents the electrooxidation of methanol on rhenium.

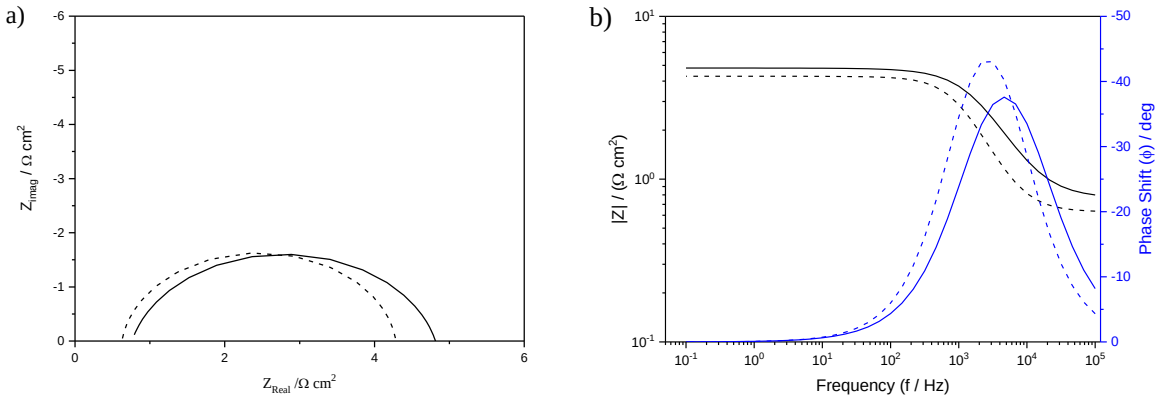

Figure 3.17. Nyquist plot and bode plot of wire electrode of metallic rhenium. The spectra were obtained at -0.3 V. Hydrogen was bubbling with stirring for 15 min beforehand in the H_2SO_4 0.5 M (solid line) and CH_3OH 1 M /H_2SO_4 0.5 M (dashed line) solutions.

Smotkin [45] suggests that metals (M) with the metal-oxygen (M-O) bond energy in the proximity to the platinum-carbon (Pt-C) bond energy, can participate in the bi-functional mechanism in alloys of platinum, see section 2.4 and Equation (Eq. 3.9).

$$CO_{(ads)} + OH_{(ads)} \rightarrow CO_{2(g)} + H^+ + e^- \qquad \text{(Eq. 3.9)}$$

In this regard, the M-O bond energy of metals of sixth period on the periodic table decreases as follow:

Ta (73) > W (74) > Re (75) > Os (76)> Ir (77) > Pt (78)

The M-O bond energy of Re (75) is higher than Pt-C bond energy and consequently rhenium is not a candidate to form an alloy with catalytic-activity.

Table 3.4. The Chi-square (χ2) values obtained by fitting the Randles (Rs(RCTC) circuit (Figure 3.14b) with Z View software,

Solutio	Potential	χ2	R_S / Ω cm^2	R_{CT} / Ω cm^2	CPE-T / sP/Ω	CPE-P
0.5 M H_2SO_4	0.00	$2.49x10^{-3}$	$0.71 \pm 7.58x10^{-3}$	9849 ± 568.19	$3.62x10^{-4} \pm 217.81$	$0.81 \pm 1.76x10^{-3}$
1 M CH_3OH	0.00	$1.42x10^{-2}$	$0.44 \pm 1.02x10^{-2}$	3858 ± 217.81	$3.27x10^{-4} \pm 8.21x10^{-6}$	$0.86 \pm 4.21x10^{-3}$
0.5 M H_2SO_4	-0.10	$5.80x10^{-3}$	$0.71 \pm 1.63x10^{-2}$	290 ± 5	$3.70x10^{-4} \pm 31.07$	$0.74 \pm 414x10^{-3}$
1 M CH_3OH	-0.10	$9.59x10^{-3}$	$0.48 \pm 9.33x10^{-3}$	1181 ± 31	$2.81x10^{-4} \pm 7.47x10^{-6}$	$0.87 \pm 4.09x10^{-3}$
0.5 M H_2SO_4	-0.13	$5.20x10^{-3}$	$0.78 \pm 1.47x10^{-2}$	121.3 ± 1.49	$3.28x10^{-4} \pm 3.99$	$0.75 \pm 4.33x10^{-3}$
1 M CH_3OH	-0.13	$4.19x10^{-3}$	$0.50 \pm 6.09x10^{-3}$	332.9 ± 3.99	$2.22x10^{-4} \pm 4.81x10^{-6}$	$0.88 \pm 3.05x10^{-3}$
0.5 M H_2SO_4	-0.20	$1.86x10^{-2}$	$0.89 \pm 1.84x10^{-2}$	23.82 ± 0.29	$1.65x10^{-4} \pm 0.23$	$0.84 \pm 8.75x10^{-3}$
1 M CH_3OH	-0.20	$1.34x10^{-2}$	$0.55 \pm 8.65x10^{-3}$	23.04 ± 0.23	$1.54x10^{-4} \pm 8.64\ x10^{-6}$	$0.90 \pm 6.55x10^{-3}$
0.5 M H_2SO_4	-0.30	$2.20x10^{-2}$	$0.76 \pm 1.21x10^{-2}$	$4.05 \pm 3.20\ x10^{-2}$	$9.78x10^{-4} \pm 3.77\ x10^{-2}$	$0.851 \pm 9.84x10^{-3}$
1 M CH_3OH	-0.30	$4.26x10^{-2}$	$0.63 \pm 1.07x10^{-2}$	$3.66 \pm 3.77x10^{-2}$	$8.74x10^{-4} \pm 1.04\ x10^{-5}$	$0.927 \pm 1.24x10^{-2}$

CPE-T is pseudo capacitance

CPE-P is related to the semi-circle in the Nyquist plot.

3.8 References

[1] Lazarescu V. Cyclic Voltammetry at Electrode Surfaces. In: Somasundaran P, editor. Encycl. Surf. Colloid Sci. 2nd ed., New York: Taylor& Francis; 2006, p. 1595–632.

[2] Mendoza J, Durán R, Genesca J. Espectroscopía de impedancia electroquímica en corrosión. In: Genesca J, editor. Técnicas electroquímicas para el Control y Estud. la Corros., Mexico City: UNAM, Facultad de Química; 2002, p. 93–118.

[3] Bard AJ, Faulkner LR. Electrochemical methods : fundamentals and applications. 2nd ed. New York: John Wiley & Sons, Inc; 2001.

[4] Chun J, Jeon S, Kim N, Chun J. The phase-shift method for determining Langmuir and Temkin adsorption isotherms of over-potentially deposited hydrogen for the cathodic evolution reaction at the poly- aqueous electrolyte interface. Int J Hydrogen Energy 2005;30:485–99. doi:10.1016/j.ijhydene.2004.12.005.

[5] Gómez J, Gardiazábal JI, Schrebler R, Gómez H, Córdova R. Electrochemical behaviour of rhenium in aqueous solution. J Electroanal Chem 1989;260:113–26. doi:10.1016/0022-0728(89)87103-7.

[6] Garcia-Garcia R, Ortega-Zarzosa G, Rincón ME, Orozco G. The Hydrogen Evolution Reaction on Rhenium Metallic Electrodes: A Selected Review and New Experimental Evidence. Electrocatalysis 2015;6:263–73. doi:10.1007/s12678-014-0240-z.

[7] Garcia-Garcia R, Rivera JG, Antaño-Lopez R, Castañeda-Olivares F, Orozco G. Impedance spectra of the cathodic hydrogen evolution reaction on polycrystalline rhenium. Int J Hydrogen Energy 2016;41:4660–9. doi:10.1016/j.ijhydene.2016.01.010.

[8] Li H, Lee K, Zhang J. Electrocatalytic H2 Oxidation Reaction. PEM Fuel Cell Electrocatal. Catal. Layers, London: Springer London; 2008, p. 135–64. doi:10.1007/978-1-84800-936-3_3.

[9] a) Skúlason E, Tripkovic V, Björketun ME, Gudmundsdóttir S, Karlberg G, Rossmeisl J, et al. Modeling the Electrochemical Hydrogen Oxidation and Evolution Reactions on the Basis of Density Functional Theory Calculations. J Phys Chem C 2010;114:18182–97. doi:10.1021/jp1048887. b) Erratum: Modeling the electrochemical hydrogen oxidation and evolution reactions on the basis of density functional theory calculations (Journal of Physical Chemistry C (2010) 114C (18182)).

[10] Santos E, Schmickler W. Electronic interactions decreasing the activation barrier for the hydrogen electro-oxidation reaction. Electrochim Acta 2008;53:6149–56. doi:10.1016/j.electacta.2007.12.049.

[11] Naor A, Eliaz N, Gileadi E, Taylor S. Properties and applications of rhenium and its alloys. AMMTIAC Q 2010;5:11–5.

[12] Grgur BN, Markovic NM, Ross PN. Electrooxidation of H2, CO and H2/CO mixtures on a well-characterized Pt-Re bulk alloy electrode and comparison with other Pt binary alloys. Electrochim Acta 1998;43:3631–5.

[13] King DL, Zhang L, Xia G, Karim AM, Heldebrant DJ, Wang X, et al. Aqueous phase reforming of glycerol for hydrogen production over Pt-Re supported on carbon. Appl Catal B Environ 2010;99:206–13. doi:10.1016/j.apcatb.2010.06.021.

[14] Hahn BP, May RA, Stevenson KJ. Electrochemical Deposition and Characterization of Mixed-Valent Rhenium Oxide Films Prepared from a Perrhenate Solution. Langmuir 2007;23:10837–45. doi:10.1021/la701504z.

[15] Vargas-Uscategui A, Mosquera E, Chornik B, Cifuentes L. Electrocatalysis of the hydrogen evolution reaction by rhenium oxides electrodeposited by pulsed-current. Electrochim Acta 2015;178:739–47. doi:10.1016/j.electacta.2015.08.065.

[16] Vladimir L. Krasikov. A new Approach to Mechanics of Hydrogen Evolution Reaction on Rhenium: 3D-Recombination,. Bull Saint Petersbg State Inst Technol (Technical Univ 2016;60:24–32. doi:10.15217/issn1998984-9.2016.34.24.

[17] Majid C a., Hussain M a. Structural transformations in polycrystalline rhenium trioxide. J Phys Chem Solids 1995;56:255–9. doi:10.1016/0022-3697(94)00173-1.

[18] Vargas-Uscategui A, Mosquera E, López-Encarnación JM, Chornik B, Katiyar RS, Cifuentes L. Characterization of rhenium compounds obtained by electrochemical synthesis after aging process. J Solid State Chem 2014;220:17–21. doi:10.1016/jossc.2014.07.043.

[19] Gaidelene J, Kuzmin A, Purans J, Guéry C. Influence of hydrogen intercalation on the local structure around Re ions in perovskite-type ReO 3. Phys Status Solidi 2005;2:149–52. doi:10.1002/pssc.200460133.

[20] Wang X, Andrews L. Matrix Infrared Spectra and Density Functional Theory Calculations of Manganese and Rhenium Hydrides. J Phys Chem A 2003;107:4081–91. doi:10.1021/jp034392i.

[21] Andreev YY. Energy profile of hydrogen evolution on metals with consideration of their surface energy. Prot Met Phys Chem Surfaces 2012;48:290–6. doi:10.1134/S2070205112030021.

[22] Appleby AJ, Chemla M, Kita H, Bronoel G, Bard A. Encyclopedia of Electrochemistry of the Elements Volume. New York, NY: M. Dekker New York; 1982.

[23] Pecherskaya AG, Stender V V. Potentials of the evolution of hydrogen in acid solutions. Zhurnal Fiz Khimii 1950;24:856–9.

[24] Krasikov VL, Varypaev VN. Electrochemical behaviour of rhenium-graphite electrode. Zhurnal Prikl Khimii 1980;53:1061–4.

[25] Joncich MJ, Stewart LS, Posey FA. Hydrogen Overvoltage on Rhenium and Niobium Electrodes. J Electrochem Soc 1965;112:717. doi:10.1149/1.2423674.

[26] Muñoz EC, Schrebler RS, Orellana M a., Córdova R. Rhenium electrodeposition process onto p-Si(100) and electrochemical behaviour of the hydrogen evolution reaction onto p-Si/Re/0.1M H2SO4 interface. J Electroanal Chem 2007;611:35–42. doi:10.1016/j.jelechem.2007.07.023.

[27] Schrebler R, Cury P, Suárez C, Muñoz E, Vera F, Córdova R, et al. Study of the electrodeposition of rhenium thin films by electrochemical quartz microbalance and X-ray photoelectron spectroscopy. Thin Solid Films 2005;483:50–9. doi:10.1016/j.tsf.2004.12.061.

[28] Trasatti S. Work function, electronegativity, and electrochemical behaviour of metals. III. Electrolytic hydrogen evolution in acid solutions. J Electroanal Chem 1972;39:163–84. doi:10.1016/S0022-0728(72)80485-6.

[29] Ferrin P, Nilekar AU, Greeley J, Mavrikakis M, Rossmeisl J. Reactivity descriptors for direct methanol fuel cell anode catalysts. Surf Sci 2008;602:3424–31. doi:10.1016/j.susc.2008.08.011.

[30] Gasteiger HA, Markov N, Ross PN, Cairns EJ. Methanol Electrooxidation on Well-Characterized Pt-Ru Alloys. J Phys Chem 1993;97:12020–9. doi:10.1021/j100148a030.

[31] Cathro KJ.a) Use of platinum-rhenium catalysts for the oxidation of aqueous methanol Electrochem Technol 1967;5:441–5, b) Low-temperature fuel cell operating on water- soluble organic fuels, Mechanical & Chemical Engineering Transactions (1967), 3(1), 17-22 and c) X-ray diffraction and electron microscope studies of narcissus mosaic virus , and comparison with potato virus X Journal of molecular biology (1967), 26(2), 353-5.

[32] Davenport WH, Kollonitsch V, Klein CH. Advances inRhenium catalysts. Ind Eng Chem 1968;60:10–9. doi:10.1021/ie50707a004.

[33] Bockris JO, Parsons R. The kinetics of the hydrogen evolution reaction at mercury cathodes. The effect of temperature, pH, and pressure on hydrogen overpotential in aqueous, mixed and methanolic solutions. Trans Faraday Soc 1949;45:916. doi:10.1039/tf9494500916.

[34] Gyenge E. Electrocatalytic Oxidation of Methanol, Ethanol and Formic Acid. PEM Fuel Cell Electrocatal. Catal. Layers, London: Springer London; 2008, p. 165–287. doi:10.1007/978-1-84800-936-3_4.

[35] Lasia A. Comments on “the phase-shift method for determining Langmuir adsorption isotherms of over-potentially deposited hydrogen for the cathodic H2 evolution reaction at poly-Re/aqueous electrolyte interfaces” [Hydrogen

Energy 30 (2005) 485-499]. Int J Hydrogen Energy 2005;30:913–7. doi:10.1016/j.ijhydene.2005.02.008.

[36] CHUN J, JEON S, KIM N, CHUN J. Response to comments on: The phase-shift method for determining Langmuir adsorption isotherms of over-potentially deposited hydrogen for the cathodic H2 evolution reaction at poly-Re/aqueous electrolyte interfaces[Hydrogen Energy 30 (2005) 485–499]. Int J Hydrogen Energy 2005;30:919–28. doi:10.1016/j.ijhydene.2005.02.007.

[37] Fuentes Quezada E. Desarrollo de materiales para pilas de combustible de metanol 2014:104.

[38] Van Loon LL, Allen HC, Wyslouzil BE. Effective Diffusion Coefficients for Methanol in Sulfuric Acid Solutions Measured by Raman Spectroscopy. J Phys Chem A 2008;112:10758–63. doi:10.1021/jp805336b.

[39] Van Loon LL, Allen HC. Methanol Reaction with Sulfuric Acid: A Vibrational Spectroscopic Study. J Phys Chem B 2004;108:17666–74. doi:10.1021/jp0476949.

[40] Rozenberg M, Loewenschuss A, Nielsen CJ. Hydrogen Bonding in the Sulfuric Acid–Methanol–Water System: A Matrix Isolation and Computational Study. J Phys Chem A 2015;119:2271–80. doi:10.1021/jp505965z.

[41] Dixit S, Poon WCK, Crain J, Dixit S, Poon WCK. Hydration of methanol in aqueous solutions: a Raman spectroscopic study. J Phys Condens Matter 2000;12:L323–8. doi:10.1088/0953-8984/12/21/103.

[42] Nikonova OA, Capron M, Fang G, Faye J, Mamede A-S, Jalowiecki-Duhamel L, et al. Novel approach to rhenium oxide catalysts for selective oxidation of methanol to DMM. J Catal 2011;279:310–8. doi:10.1016/j.jcat.2011.01.028.

[43] Chan ASY, Chen W, Wang H, Rowe JE, Madey TE. Methanol Reactions over Oxygen-Modified Re Surfaces: Influence of Surface Structure and Oxidation †. J Phys Chem B 2004;108:14643–51. doi:10.1021/jp040168x.

[44] Anderson AB, Grantscharova E, Seong S. Systematic Theoretical Study of Alloys of Platinum for Enhanced Methanol Fuel Cell Performance. J Electrochem Soc 1996;143:2075–82. doi:10.1149/1.1836952.

[45] Smotkin ES. Chapter 8 – FTIR and X-ray Absorption Spectroscopy of Operating Fuel Cells. In-situ Spectrosc. Stud. Adsorpt. Electrode Electrocatal., 2007, p. 247–72. doi:10.1016/B978-044451870-5/50009-9.

Chapter IV

Conclusions

A discussion with the studies reported on the literature to understand the electroactivity for the Hydrogen Oxidation Reaction (HOR) and Hydrogen rhenium Evolution Reaction (HER) on rhenium was established on chapter 1. The experimental work was developed using a rhenium electrode obtained by metallurgical techniques. The results found show different values compared with what it is reported in the literature, in which electrodes obtained by the electrodeposition of soluble oxide were used.

The following points have been shown:

1. The exchange current density of HER on rhenium is $1.6\times10^{-6} \pm 2.43\times10^{-6}$ Acm^{-2}. The experimental part was explored until -0,4V vs NHE as of cathodic potentials.
2. The Tafel slope determined for HER on rhenium is 60 $mVdecade^{-1}$ at lower overpotentials.
3. It can be postulated that the rhenium obtained by metallurgical processes follows the Sabatier principle.
4. The two different adsorption energies of Hydrogen on metallic rhenium were not observed by electrochemical impedance spectroscopy and the potential–log (*j*) current plots. Then, the mechanism proposed for HER on electrodeposited rhenium is difficult to observe in the HER on metallurgical (fused) rhenium electrode at low polarization potentials.
5. The soluble of rhenium (VI) oxide influences insignificantly the Hydrogen Evolution Reaction.
6. Several values for the work function (Φ) and exchange current density (j_0) for HER are reported for the sixth period metals in the periodic table. Some of these values produce a linear relation between log j_0 values and the metal work functions (Φ). This linear plot can be generated using the following selected values of Φ-coordinate and log j_0-coordinate: Ta (73) (4.23 eV, -8.15), W (74) (4.55 eV, -6.4), Re (75) (4.87 eV,-5.79), Os (76) (5.24 eV,-4.05), Ir (77) (5.3 eV, -3.71), Pt (78) (5.64 eV, -2.73).

7. The work function of platinum is higher than rhenium, from this comparison it is possible to suggest that the reported j_0 values for HER on rhenium cannot therefore be supported.

8. The rhenium voltammogram in acid media dissolutions does not show the hydrogen underpotential deposition (H-UPD).
9. The HOR and the HER are not reversible reactions on rhenium.
10. The equivalent circuit Randles described the behavior of the HER on rhenium electrode at low cathodic potential. This Randles equivalent circuit can describe the comportment of impedance spectra in acid solutions with or without methanol.
11. The theoretical predictions on studies reported about a stepwise dehydrogenation of methanol on rhenium, between 0.4-0.8 V are not confirmed by the results obtained. In addition, the methanol electrooxidation on metallic rhenium does not occur at low or high methanol concentrations, so does nor participate in the bi-fuctional mechanism.
12. In brief, the influence of methanol in the HER on metallic rhenium is lower compared to platinum metals group.

As can be expected new issues are still unknown and consequently in further investigation the following topics must be investigated:

a) The mean enthalpy of activation at the equilibrium potential could be related to the forward and backward steps of the Tafel reaction, it is necessary obtain experimental result to supported.
b) The HER and HOR on rhenium in basic media is not yet investigated, as in platinum exists the exchange current values for HER and HOR, it is necessary obtain more experimental results for rhenium in this media to contribute with more knowledge to understand the rhenium as electrocatalyst.

Appendix A

Table A.1 Values obtained by fitting the Randles ($Rs(R_{CT}C)$) circuit with Z View software for different measurements at 0.00 V.

	1			2			3			4		
Element	Valor	Error	Error %	Valor	Error	Error %	Valor	Error	Error %	Valor	Error	Error %
R_S	0.708	0.008	1.070	0.831	0.010	1.186	0.436	0.010	2.346	0.501	0.009	1.883
R_{CT}	9849.000	568.189	5.769	12852.000	876.879	6.823	3858.000	217.811	5.646	5734.000	368.650	6.429
CPE-T	0.000	0.000	1.023	0.000	0.000	1.192	0.000	0.000	2.512	0.000	0.000	1.980
CPE-P	0.809	0.002	0.217	0.825	0.002	0.251	0.861	0.004	0.488	0.853	0.003	0.398

Table A.1 Values obtained by fitting the Randles ($Rs(R_{CT}C)$) circuit with Z View software for different measurements at -0.10 V.

	1			2			3			4		
Element	Valor	Error	Error %	Valor	Error	Error %	Valor	Error	Error %	Valor	Error	Error %
R_S	0.714	0.016	2.283	0.840	0.011	1.359	0.479	0.009	1.948	0.512	0.010	1.939
R_{CT}	289.600	5.004	1.728	5208.000	183.301	3.520	1181.000	31.074	2.631	1797.000	55.421	3.084
CPE-T	0.000	0.000	3.075	0.000	0.000	1.399	0.000	0.000	2.655	0.000	0.000	2.312
CPE-P	0.739	0.004	0.560	0.807	0.002	0.287	0.866	0.004	0.472	0.848	0.004	0.438

Table A.1 Values obtained by fitting the Randles ($Rs(R_{CT}C)$) circuit with Z View software for different measurements at -0.13 V.

	1			2			3			4		
Element	Valor	Error	Error %	Valor	Error	Error %	Valor	Error	Error %	Valor	Error	Error %
R_S	0.779	0.015	1.892	0.854	0.009	1.096	0.503	0.006	1.211	0.534	0.007	1.313
R_{CT}	121.300	1.488	1.227	1450.000	20.078	1.385	332.900	3.986	1.197	444.900	5.857	1.316
CPE-T	0.000	0.000	3.425	0.000	0.000	1.379	0.000	0.000	2.162	0.000	0.000	2.131
CPE-P	0.748	0.004	0.579	0.814	0.002	0.257	0.884	0.003	0.345	0.871	0.003	0.353

Table A.1 Values obtained by fitting the Randles ($Rs(R_{CT}C)$) circuit with Z View software for different measurements at -0.2 V.

	1			2			3			4		
Element	Valor	Error	Error %	Valor	Error	Error %	Valor	Error	Error %	Valor	Error	Error %
R_S	0.891	0.018	2.061	0.929	0.014	1.540	0.547	0.009	1.582	0.568	0.009	1.554
R_{CT}	23.820	0.294	1.234	62.660	0.625	0.998	23.040	0.233	1.010	25.360	0.252	0.992
CPE-T	0.000	0.000	7.589	0.000	0.000	4.354	0.000	0.000	5.592	0.000	0.000	5.323
CPE-P	0.837	0.009	1.046	0.841	0.005	0.623	0.898	0.007	0.729	0.891	0.006	0.702

Table A.1 Values obtained by fitting the Randles ($Rs(R_{CT}C)$) circuit with Z View software for different measurements at -0.3 V.

	1			2			3			4		
Element	Valor	Error	Error %	Valor	Error	Error %	Valor	Error	Error %	Valor	Error	Error %
R_S	0.761	0.012	1.587	0.973	0.016	1.610	0.628	0.011	1.704	0.553	0.010	1.750
R_{CT}	4.053	0.032	0.790	9.874	0.082	0.832	3.658	0.038	1.031	2.863	0.028	0.961
CPE-T	0.000	0.000	9.752	0.000	0.000	8.434	0.000	0.000	11.889	0.000	0.000	11.835
CPE-P	0.851	0.010	1.156	0.890	0.009	0.984	0.927	0.012	1.337	0.904	0.012	1.327